NASA TECHNICAL NOTE

NASA TN D-5853
c. 1

GUIDANCE AND CONTROL PAYLOAD SUPPORT REQUIREMENTS FOR A PLANETARY CARTOGRAPHIC PROBE

by Saul Moskowitz

Electronics Research Center
Cambridge, Mass. 02139

RECEIVED
1 JUL 1970
Technical Library
AF Weapons
Laboratory

NATIONAL AERONAUTICS AND SPACE ADMINISTRATION • WASHINGTON, D. C. • JUNE 1970

1. Report No. NASA TN D-5853	2. Government Accession No.	3. Recipient's Catalog No.
4. Title and Subtitle GUIDANCE AND CONTROL PAYLOAD SUPPORT REQUIREMENTS FOR A PLANETARY CARTOGRAPHIC PROBE		5. Report Date June 1970
		6. Performing Organization Code
7. Author(s) Saul Moskowitz		8. Performing Organization Report No. C-109
9. Performing Organization Name and Address Electronics Research Center Cambridge, Mass.		10. Work Unit No.
		11. Contract or Grant No. 125-17-02-02
		13. Type of Report and Period Covered
12. Sponsoring Agency Name and Address National Aeronautics and Space Administration		Technical Note
		14. Sponsoring Agency Code

15. Supplementary Notes

16. Abstract

The guidance and control requirements for payload support of a planetary orbiting cartographic spacecraft have been examined. Mapping scales of $1:10^6$ and $1:5 \times 10^6$ (with their associated accuracy and resolution specifications) were selected for the parametric study of Lunar, Martian, and Jovian cartography. Relations were established between camera pointing angle, field-of-view, and imaging resolution in terms of planetary physical characteristics and mapping scale. From these, orbit selection rules were formulated for orbits of various inclinations with particular attention directed towards those of 30 and 90 degrees (polar orbits). Spacecraft attitude control requirements were then obtained as a function of these parameters and the selected image overlap. The resulting overall guidance and control specifications are described in terms of potential instrumentation sussystems.

17. Key Words • Lunar, Martian, Jovian Cartography • Camera Pointing Angle • Field-of-view • Imaging Resolution Potential • Instrumentation Sub-systems	18. Distribution Statement Unclassified-Unlimited		
19. Security Classif. (of this report) Unclassified	20. Security Classif. (of this page) Unclassified	21. No. of Pages 43	22. Price* $3.00

GUIDANCE AND CONTROL PAYLOAD SUPPORT REQUIREMENTS
FOR A PLANETARY CARTOGRAPHIC PROBE

By Saul Moskowitz
Electronics Research Center

SUMMARY

The guidance and control requirements for payload support of a planetary orbiting cartographic spacecraft have been examined. Mapping scales of $1:10^6$ and $1:5 \times 10^6$ (with their associated accuracy and resolution specifications) were selected for the parametric study of Lunar, Martian, and Jovian cartography. Relations were established between camera pointing angle, field-of-view, and imaging resolution in terms of planetary physical characteristics and mapping scale. From these, orbit selection rules were formulated for orbits of various inclinations with particular attention directed towards those of 30 and 90 degrees (polar orbits). Spacecraft attitude control requirements were then obtained as a function of these parameters and the selected image overlap. The resulting overall guidance and control specifications are described in terms of potential instrumentation subsystems.

INTRODUCTION

Two distinct classes of guidance, navigation, and control requirements can be identified with respect to missions for the direct scientific exploration of the solar system. The first is that class associated with the transportation of the scientific payload to those regions of space where the desired observations and measurements are to be performed. The second class of requirements consists of those related to the support of the payload during its operation. The effort described in this report was directed towards this latter class as applied to a specific mission; that of producing quantitative maps of the various bodies of the solar system.

Early studies of lunar problems (ref. 1), as refined after the subsequent receipt of additional space derived data (ref. 2), led the author and his associates to an examination of the pointing control problem for a lunar orbiting, multiaspect, high resolution telescopic camera (ref. 3). The data presented herein represent an extension of these initial efforts. First, to a determination of the guidance, navigation and control requirements for a lunar orbiting, cartographic (photo-mapping) spacecraft. Secondly, to the general case of a planetary cartographic orbiter. (The analysis of the lunar cartography problem was formulated in terms of the requirements established in Chapter 7, reference 2.)

The approach adopted for this effort differs from those of earlier studies (refs. 4 and 5) in that here cartographic imaging is formulated parametrically rather than in terms of specific equipment or equipment classes. First, mapping scales, and their associated

resolutions and accuracies, were selected. Then by specifying a range of image resolutions and considering both nadir and oblique pointing cameras, optical field-of-view was related to altitude over the given range of variables. Derived orbit quantization levels (so that complete planetary coverage would be achieved) combined with the above mentioned data permitted the selection of specific orbits about each of the planets and the Earth's moon. To aid in the generation of actual guidance and control requirements and constraints, several representative guidance, navigation, and control (GN&C) systems were postulated at the schematic level. Thus, a range of GN&C parameters was derived with respect to the basic cartographic requirements in terms of practical equipment configurations. These, when compared to the state-of-the-art of instrumentation, should then aid the specification of feasible mission parameters compatible with equipment capabilities.

MAPPING PARAMETERS

The mission objective of any cartographic operation is generating sufficient data to permit the compilation of maps of metric quality. By "metric quality" one infers specified orthographic linearities and positional accuracies, elevation contour spacing and accuracy, and horizontal and vertical resolutions. Camera design parameters can be generated from these numbers and the special facts of the mapping operation (e.g., the physical properties of the selected planet; its mass, surface radius, atmospheric structure, diurnal period, polar axis orientation, period of revolution about the Sun, etc.). The metric quality of cartographic imagery is normally given in terms of mapping scale.

Mapping Scales

The scale of a map is the ratio of displayed image size to object size. Associated with each scale, one specifies a ground plane resolution, a positional accuracy with respect to a geodetic control network, the contour interval, and an accuracy of elevation determination (all in linear measure). As Doyle points out with respect to lunar cartography (ref. 4):

"The ground resolution required for compiling terrestrial maps is dictated primarily by the cultural features (roads, buildings, etc.) which must be included. These are nearly independent of map scales, and hence required resolution is not linearly related to map scale. On the Moon, however, cultural features are expected to be absent so that a linear relation seems justified."

Extending this reasoning to the general case of planetary mapping accuracy requirements as a function of map scale means using the values given in Table I. Data for mapping scales 1:10,000 through 1:2,500,000 are from ref. 4, while the 1:5,000,000 case was obtained by linear extrapolation.

2

TABLE I.- MAPPING ACCURACY REQUIREMENTS

Map Scale	Position Accuracy (Meters, rms)	Ground Resolution (Meters)	Contour Intervals (Meters)	Elevation Accuracy (Meters, rms)
$1:5 \times 10^6$	1500	250	2000	750
$1:2.5 \times 10^6$	750	125	1000	375
$1:10^6$	300	50	500	150
$1:2.5 \times 10^5$	75	12.5	100	30
$1:10^5$	30	5.0	50	15
$1:5 \times 10^4$	15	2.5	25	8
$1:2.5 \times 10^4$	7.5	1.3	10	3
$1:10,000$	3.0	0.5	5	1.5

For mapping scale selection criteria, reference is made to the report of the Lunar Science Geodesy & Cartography Working Group (ref. 2). For the Moon, the following sets of maps are listed:

1. Orthographic, Mercator, and polar stereographic projections of the whole Moon, 1:5,000,000 scale

2. Complete coverage of the Moon, 1:1,000,000 scale

3. Coverage of approximately 20 areas of interest as Apollo Applications Program (AAP) landing sites and traverses, 1:250,000 scale

4. Coverage of central parts of 20 areas of special interest, 1:50,000 scale

5. Coverage of landing sites in the central portion of AAP sites, 1:5,000 scale

Considering the preliminary form of this present study, the mapping sets describe under items 1 and 2 (above) were selected for extension to the general case of planetary cartography. Thus the following analyses have been based upon $1:5 \times 10^6$ and $1:10^6$ mapping scales as defined in Table I. In retrospect, it should be noted that the Lunar Astronautical Chart (LAC) series of maps of the near-side of the lunar surface produced for NASA by the U.S. Air Force Aeronautical Chart and Information Center were drawn from earth-based observations to the scale of $1:10^6$. Lunar Orbiter data was used similarly to prepare lunar far-side maps at a scale of $1:5 \times 10^6$.

Camera field-of-view can be expressed in terms of spacecraft altitude as a function of map scale. Object plane field size is related to object plane resolution element size through the selection, or limitations, of image resolution. Several approaches to imaging system design have been considered, some of which have been applied to lunar study (ref. 6). However, so as not to constrain the present study more than necessary, image resolution was used as a design parameter in the form of n lines per side of a square image field. This is ideal if image tube systems are to be employed. For photographic film n is the product of the number of lines of image resolution per linear measure multiplied by the length of the side of the film. Here, for numerical calculations, five values of n were employed: n = 500, 1000, 2000, 3000, and 4000. Thus (as shown in Figure 1) if the curved planetary surface is approximated by a plane (so that the results obtained are approximately valid for all the planets) the size of the image field in the object plane is n(δs) where (δs) is ground resolution as listed in Table I. Object plane field sizes are listed in Table II for the two selected mapping scales and the five values of n.
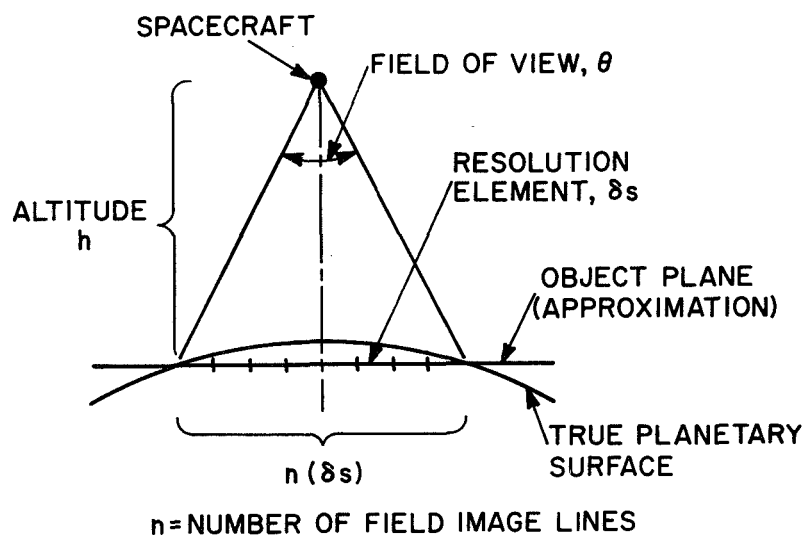

Figure 1.- Geometry of object plane approximation

TABLE II.- OBJECT PLANE SIZE OF FIELD

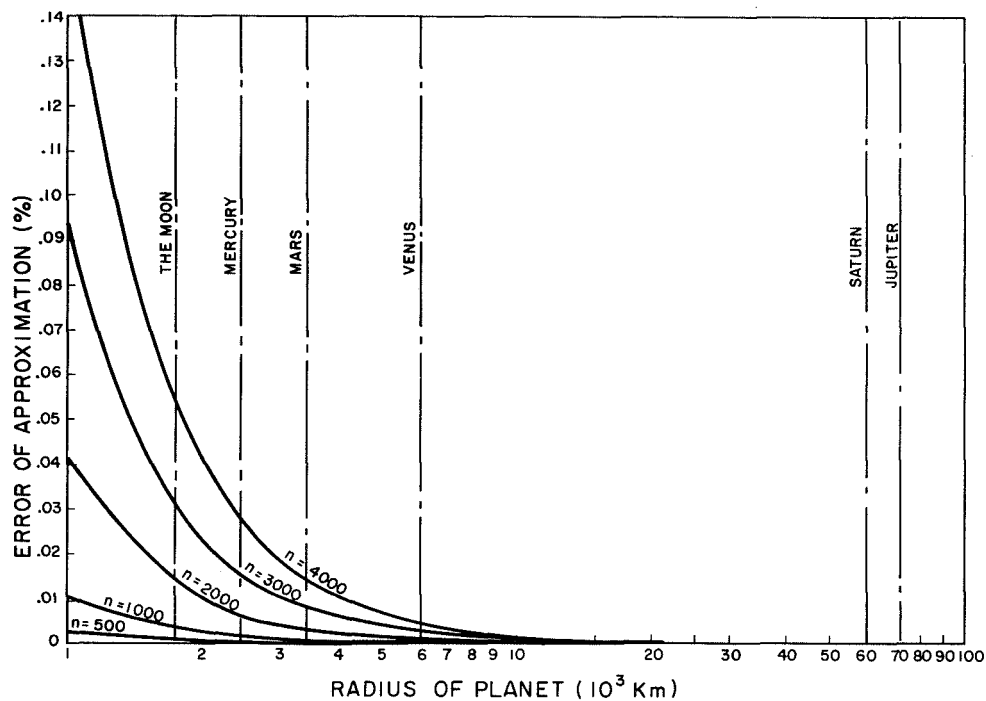| Map Scale	Image Resolution (n)				
	500 lines	1000 lines	2000 lines	3000 lines	4000 lines
$1:10^6$	25 Km	50 Km	100 Km	150 Km	200 Km
$1:5 \times 10^6$	125 Km	250 Km	500 Km	750 Km	1000 Km

4

Figure 2.- Field of view excess due to flat planet
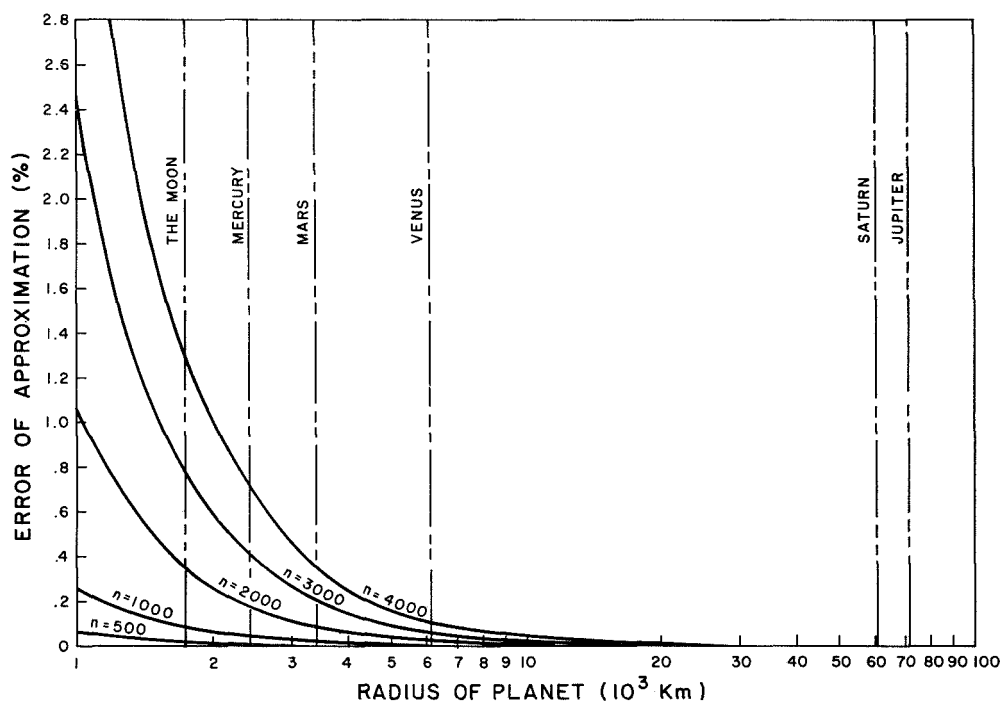approximation — $1:10^6$ scale mapping

Figure 3.- Field of view excess due to flat planet
approximation — $1:5 \times 10^6$ scale mapping

The limits of the validity of the flat planet approximation are shown by Figure 2 (1:10^6 mapping scale) and Figure 3(1:5 x 10^6 mapping scale). The flat planet approximation results in the calculated field-of-view being in excess of the true required field-of-view. Correspondingly, ground image resolution is decreased in approximately the same proportion if the number of image lines (n) is held constant. The curves of Figure 2 indicate that the indicated approximation produces, at worst, an error of no greater than about 0.05 percent (1 part in 2000) for the Moon at 1:10^6 scale mapping. The error is somewhat less for the various planets. In the case of 1:5 x 10^6 scale mapping the errors are somewhat larger (Figure 3). However, since maps of the Moon already exist at 1:5 x 10^6 scale, the errors of the flat planet approximation do not exceed 0.8 percent for any planet of interest and are negligible for Jupiter and Saturn.

Elevation Accuracy Resultant Constraints

Normally a nadir point camera approach would be chosen for obtaining cartographic images because of resultant lack of system complexity. A single camera (Figure 4) may be employed to obtain overlapping stereoscopic images from which elevation information may
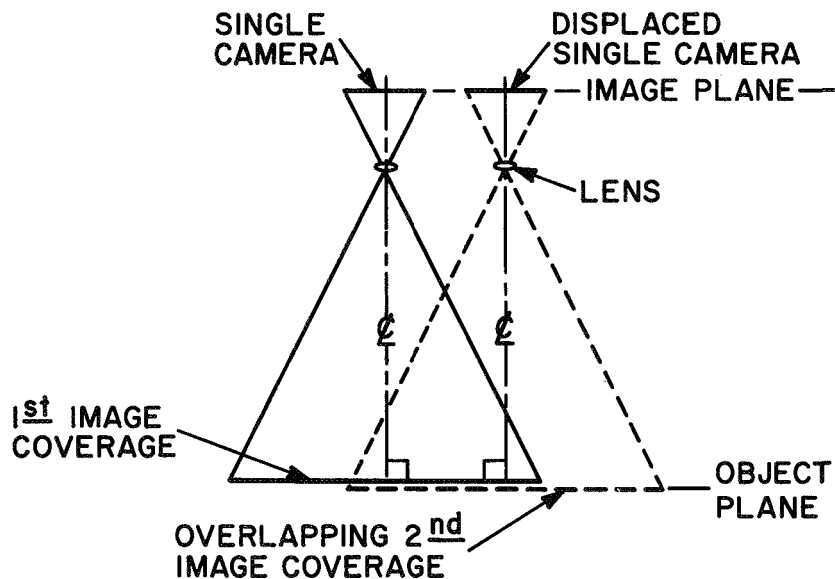

Figure 4.- Nadir pointing single camera

be obtained. However, as camera altitude increases (with fixed object size) field-of-view decreases and so camera separation between successive exposures must decrease until an insufficient stereo base length results for a desired vertical accuracy. Then oblique pointing cameras must be employed (Figure 5). Two cameras are now required

instead of one (with a corresponding increase in system complexity).
The point at which this cross-over occurs is derived in the following
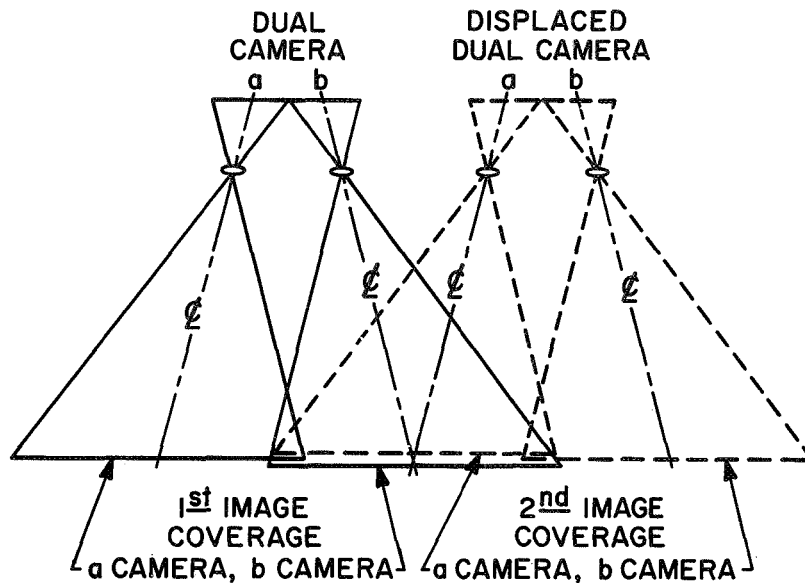paragraphs.

Figure 5.- Oblique pointing dual camera

For the nadir pointing situation, camera translation distance,
camera altitude, and image resolution determine the accuracy of object
elevation determination. The elevation error triangle of Figure 6
represents the uncertainty distribution in elevation, e, of a parti-
cular point imaged on distinct surface plane resolution elements from
a pair of overlapping images.

If ℓ = translation of spacecraft between images

   K = overlap fraction (e.g.,.60 or 60%)

   s = position of target from nadir in horizontal plane

(δs) = surface resolution element

 $\theta/2$ = camera half-angle

   h = altitude of spacecraft

   e = elevation of object point

(δe) = maximum value of error in elevation

   ϕ_1, ϕ_2, as defined in Figure 6a, then

$$\ell = (1-K)\ 2h\ \tan\ \theta/2 \qquad (1)$$

$$\tan\ \phi_1 = \frac{s}{h-e} \qquad (2)$$

$$\tan\ \phi_2 = \frac{\ell-s}{h-e} \qquad (3)$$

Approximating the elevation error triangle by Figure 6b (valid for small values of the ratio $(\delta s)/n(\delta s)$ or $1/n$)

$$\tan\ \phi_1 = \frac{\mu}{(\delta e)}\ (\delta s) \qquad (4)$$

$$\tan\ \phi_2 = \frac{(1-\mu)}{(\delta e)}\ (\delta s)\ \frac{h-e}{h} \qquad (5)$$
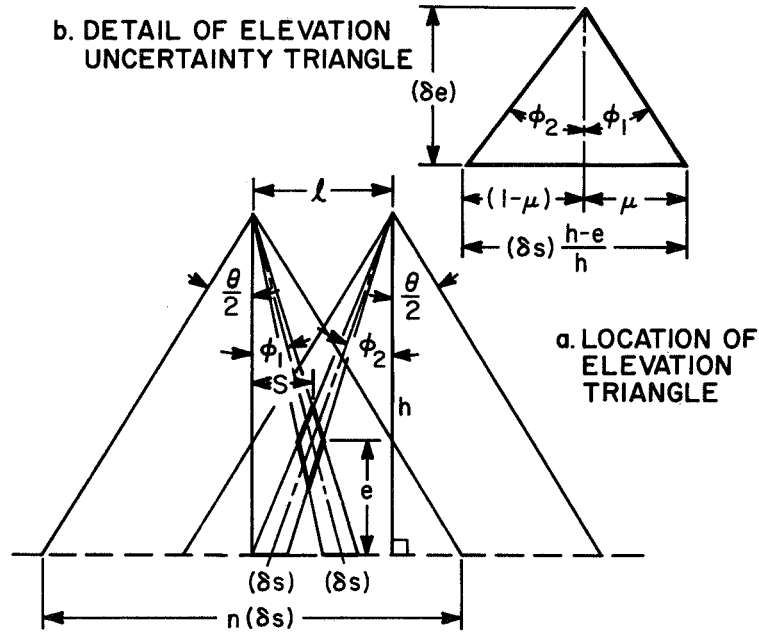
Figure 6.- Geometry of object elevation uncertainty for nadir pointing cameras

Now (δe) is directly proportional to $(h-e)$, as is shown by Eqs. (2) and (4) or Eqs. (3) and (5), and takes on a maximum value for $e = 0$ (object in the ground plane). For this maximum error case

$$\tan\ \phi_1 = \frac{s}{h} = \frac{\mu}{(\delta e)}\ (\delta s) \qquad (6)$$

$$\tan\ \phi_2 = \frac{(1-K)\,2h\ \tan\ \theta/2\ -s}{h} = \frac{(1-\mu)}{(\delta e)}\ (\delta e) \qquad (7)$$

Solving (6) and (7) for the ratio $\delta e/\delta s$

$$\frac{\delta e}{\delta s} = \frac{1}{(1-K)2 \tan \theta/2} \tag{8}$$

Thus, the elevation error is independent of s and constant across the entire object plane. Dependency upon spacecraft altitude and camera separation has been replaced by dependency upon θ, the camera angular field-of-view. For a limiting value of $\delta e/\delta s$, a limiting value for θ may be obtained.

$$\theta = 2 \arctan \frac{1}{\frac{\delta e}{\delta s} 2 (1-K)} \tag{9}$$

A numerical value for $\delta e/\delta s$ is obtained from Table I which gives

$$\frac{(\delta e)_{rms}}{(\delta s)} = 3 \tag{10}$$

for both mapping scales under consideration. It can be shown that for the given triangular distribution (of Figure 6b)

$$(\delta e)_{rms} = .41 \delta e \tag{11}$$

Then inserting Eq. (10) and Eq. (11) in Eq. (9), the limiting value of θ becomes

$$\theta_{min} = 18.9 \ deg \tag{12}$$

Equation (12) states that to meet the required elevation accuracies given in Table I, no combination of spacecraft altitude, ground plane object size, image overlap, and camera displacement between exposures is permitted which will result in a value of field-of-view for the nadir pointing camera of less than 18.9 degrees. To avoid this limitation, it becomes necessary to employ oblique pointing cameras.

The problem of oblique pointing is that of the determination of the minimum offset angle α (of Figure 7) which maintains the same lateral camera displacement-altitude ratio which yields the elevation error triangle defined by Eq. (10) and Eq. (11). Substituting Eq. (8) into Eq. (1)

$$\ell = h / \frac{\delta e}{\delta s} \tag{13}$$

From Figure 7

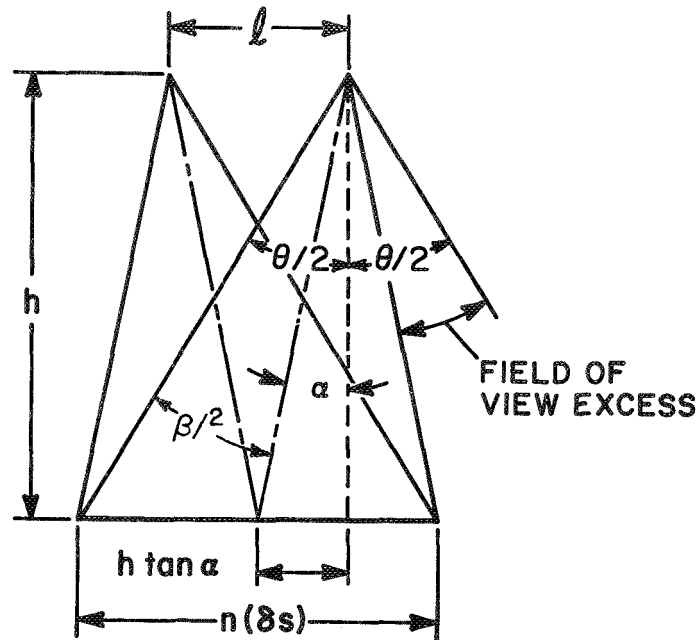$$\tan \alpha = \frac{\ell/2}{h} = \frac{1}{2} \frac{\delta s}{\delta e} \tag{14}$$

Figure 7.- Geometry of the oblique pointing camera

using Eq. (10) and Eq. (11)

$$\alpha \approx 3.8 \text{ deg} \tag{15}$$

Camera Fields-of-View

Parametric relations between mapping scale, spacecraft altitude, image resolution number (n), and camera angle combined with the constraints given by Eq. (12) for the nadir pointing case will establish the permitted range of solutions for planetary mapping. From Figure 6a, for the nadir pointing case (planar approximation).

$$\theta = 2 \arctan \frac{n(\delta s)}{2h} \tag{16}$$

where θ is the camera field-of-view. Optical design limitations place an upper bound on θ of about 90 degrees. Using Eq. (16) Figures 8 and 9 have been prepared for the $1:10^6$ and $1:5 \times 10^6$ mapping scale cases, respectively. It is interesting to note that only a small range in spacecraft altitude exists (in both cases) between the minimum and maximum values of camera field-of-view.
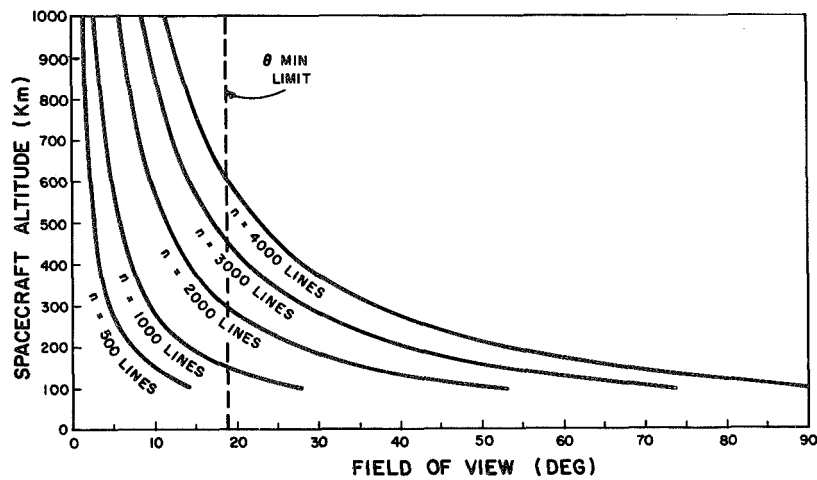
Figure 8.- Field-of-view curves for $1:10^6$ scale mapping (nadir pointing camera)
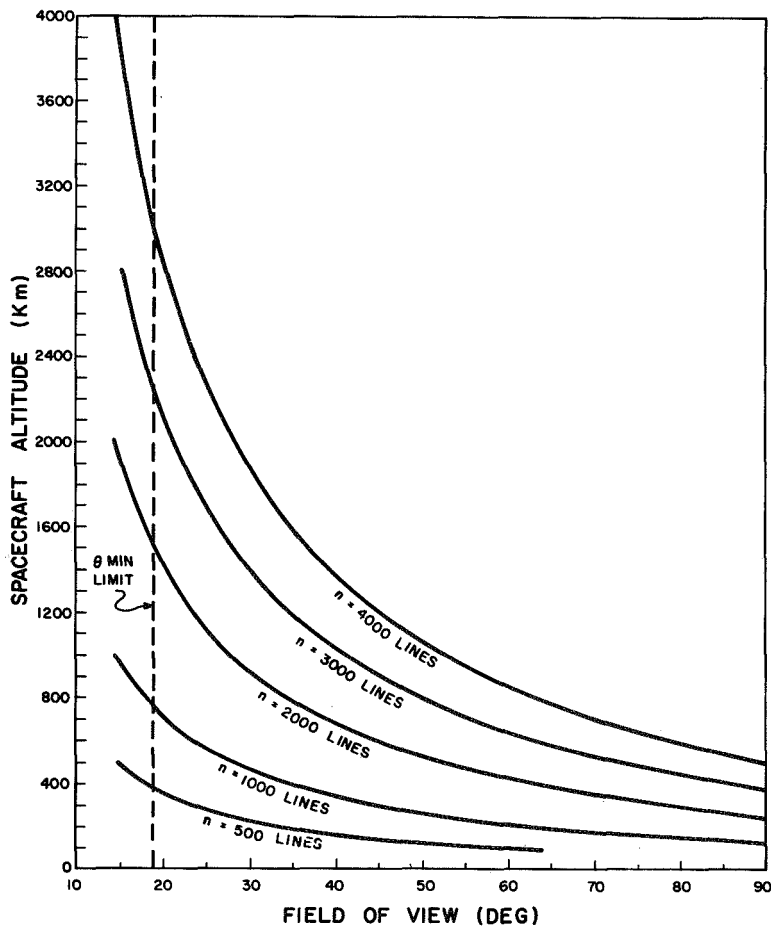

Figure 9.- Field-of-view curves for $1:5 \times 10^6$ scale mapping (nadir pointing camera)
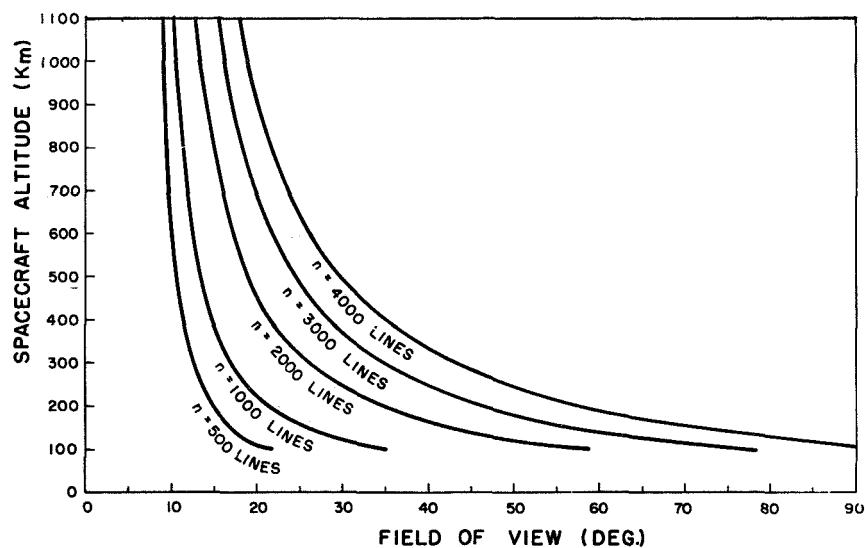
Figure 10.- Field-of-view curves for $1:10^6$ scale mapping
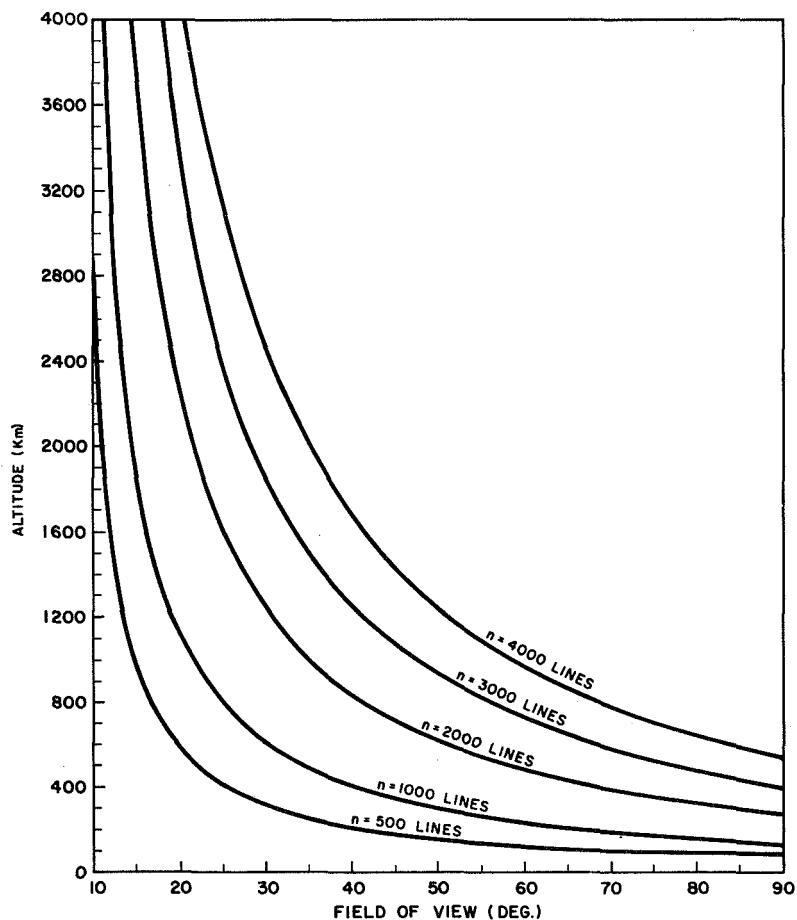(3.8 deg oblique pointing camera)

Figure 11.- Field-of-view curves for $1:5 \times 10^6$ scale mapping
(3.8 deg oblique pointing camera)

12

PHYSICAL PROPERTIES

Physical data for the planets and the Moon, as required for a first-order analysis, are presented in Table III. A simple spherical model of mass distribution is used for all the planets. Spacecraft orbits were calculated on this basis even though Jupiter and Saturn exhibit (optically) oblateness on the order of 1/15 and 1/10, respectively. Of the three bodies receiving detailed study (Moon, Mars, and Jupiter), Jupiter presents particular problems to any cartographic operation. A clearly defined visible surface exists for the Moon and Mars. Jupiter's surface, if it exists at all, is hidden by a dense, cloudy atmosphere.

The equatorial radius of Jupiter given in Table III is the measurement to the top of the observed cloud cover. The latitude dependence of this radius is listed in Table IV. No observations have ever been made of the surface of Jupiter. Theoretical models of the Jovian atmosphere give estimates of the depth from the top of the cloud cover to something like a surface as great as 4250 km (Ch. 14, ref. 9). The deep atmosphere models indicate surface temperatures of about 2000°K and a pressure of 200,000 earth atmospheres. It is doubtful if any optical system operating in or near the visual region of the spectrum would be able to penetrate very far into such an atmosphere. Thus, cartography of Jupiter will probably be restricted to recording and measuring the cloud structure at or near the top of the cloud layer; a structure which shows variation with time.

All information to date shows that the Moon has essentially no atmosphere. Thus, there are really no limitations on the closeness of an orbiting spacecraft to the lunar surface except those required to prevent orbital perturbations from causing the spacecraft to impact the surface. This same situation is almost true for Mars. Models based upon Mariner IV results (ref. 8) yield a surface pressure of only 5 to 10 millibars or between about 1/200 and 1/100 of an earth atmosphere.

A spacecraft at an orbital altitude of greater than 200 km from the surface of Mars should experience negligible drag. Jupiter, however, again presents a significantly different situation. It is now assumed that the pressure at the top of the cloud cover lies somewhere between 1 and 3 earth atmospheres (ref. 9). The pressure (or density) structure above this surface is still somewhat uncertain. For the purposes of the following analyses, a lower altitude constraint of 600 km above the equatorial cloud top has been placed upon orbit selection.

For the oblique pointing case (planar approximation) use of Figure 7 yields

$$\theta = 2 \ (\alpha + \beta/2) = 2 \ \text{arctan} \quad \text{tan} \ \alpha + \frac{n(\delta s)}{2h} \tag{17}$$

It should be noted that θ now is the total field angle of the camera lens and as such covers more than the image field-of-view. This situation results from a desire to maintain the image plane parallel to the object plane so that image motion compensation can be achieved through a uniform rate of image plane translation. Thus the image centerline is offset from the optical axis by the angle α. Using Eq. (17), Figures 10 and 11 have been prepared for the $1:10^6$ and $1:5 \times 10^6$ mapping scale cases, respectively. The 90-degree maximum field of view limit (optical design restriction) still applies. However, with the oblique pointing configuration, the minimum field limits are those which result from camera pointing accuracy and stabilization limitations and eventually from diffraction effects.

PLANETARY CHARACTERISTICS

The analytical results discussed previously in MAPPING PARA-METERS are completely general (using the flat objet plane approximation where required) and are applicable to any planetary mapping operation. The "special facts" of particular bodies are now required to continue this development. The reference planetoid is needed so that the number of image fields about the equator for each mapping scale and resolution number can be determined. The gravitation field is used to calculate the period of particular orbits about the planet. Then selection rules can be derived which yield those permitted values of the ratio between the siderial diurnal period of the planet and the orbital period of the spacecraft which produce complete and unique mapping coverage. These selection rules are also a function of the inclination of the orbit. General results are presented for the Moon and all the planets from Mercury through Saturn in order to illustrate the development of such relations. Detailed results are presented for the Moon, Mars, and Jupiter.

14

TABLE III.- CHARACTERISTICS OF THE PLANETS AND THE MOON[*]

Body	Equatorial Radius (km)	Equatorial Circumfer-ence (km)	Diurnal Period (siderial)	Period of Revolution (siderial)	Gravitational Constant (km^3/sec^2)
Moon	1,738	10,920	27.322 days	27.322 (days)	4,904
Mercury	2,420	15,205	59 ± 2 days	0.2411	21,800
Venus	6,100	38,327	242.6 ± .6 days[**]	0.6156	324,850
Mars	3,395	21,331	24 h 37.38 m	1.8822	42,930
Jupiter	71,387	448,537	9 h 50 m[†]	11.86	1.2671×10^8
Saturn	60,400	379,504	10 h 14 m	29.46	3.792×10^7

[*]Data derived from refs. 7, 8, and 9
[**]Retrograde motion
[†]System I, equatorial region

TABLE IV.- RADIUS OF JUPITER AT VARIOUS LATITUDES[*]

Zenocentric Latitude	Radius of Visible Glove (km)
0°	71,387
15°	71,094
30°	70,295
45°	69,204
60°	68,825
75°	67,313
90°	67,020

[*]Taken from Table 3-2 of Reference 9

The studies of Karrenberg, Levin, and Lüders (Ref. 10) have
resulted in detailed orbit synthesis constraints and requirements for
Earth-orbiting satellites. Their formulation of the problem appears
sufficiently general for extension to various problems of planetary
orbiters with observational subsystems. They consider problems of
imagery coverage (both complete and partial), orbital precession
and change due to oblateness of the gravitational field and atmos-
pheric drag, illumination angle, orbital ellipticity, and orbital
maintenance and transfer. Here, in order to establish preliminary
guidance and control requirements, a particularly restricted problem
is considered. It is assumed that the orbits are nominally circular,
the gravitational field is spherically symmetrical, and that, to
first order, the orbits lie above the sensible atmosphere. (Upper
limits on these same orbits are those established by Figures 8, 9,
10, and 11.) The selection rules which will yield those orbits
resulting in complete, and unique mapping coverage are derived below.
They prove consistent with the work of Karrenberg, Levin, and Lüders,
in that they are a special case of more general relations.

The width and length of the square image frame on the (assumed
flat) ground plane is $n(\delta s)$ or the product of the number of image
lines and the specified ground resolution element. The arbitrary
specification of the orientation of this image frame so that one side
is parallel with the instantaneous orbital plane permits the deriva-
tion of the required relations for complete mapping coverage. If C_E
is the equatorial circumference of the planet, N, the number of orbital
passes needed to give complete coverage from polar orbit is

$$N = \left[\frac{C_E}{0.9n(\delta s)}\right]' \tag{18}$$

where the prime (') indicates the next highest integer value and a
10 percent overlap yields the 0.9 multiplying factor. Other values
of overlap may be chosen depending upon the outcome of the tradeoff
between number of data elements and spacecraft stabilization accuracy.
Figure 12a depicts these overlapping image frames equally spaced about
the planetary equator.

The problem of spacing oblique orbits, orbits with inclinations
less than 90 degrees, yields more complicated expressions. Based
upon spherical trigonometry, the exact expression for the equatorial
spacing, D, between adjacent orbital passes is

$$D = 2 R_E \arcsin\left(\frac{\sin\dfrac{0.9\ n(\delta s)}{2R_E}}{\sin i}\right) \tag{19}$$

where R_E is the mean equatorial radius of the planet and i is the
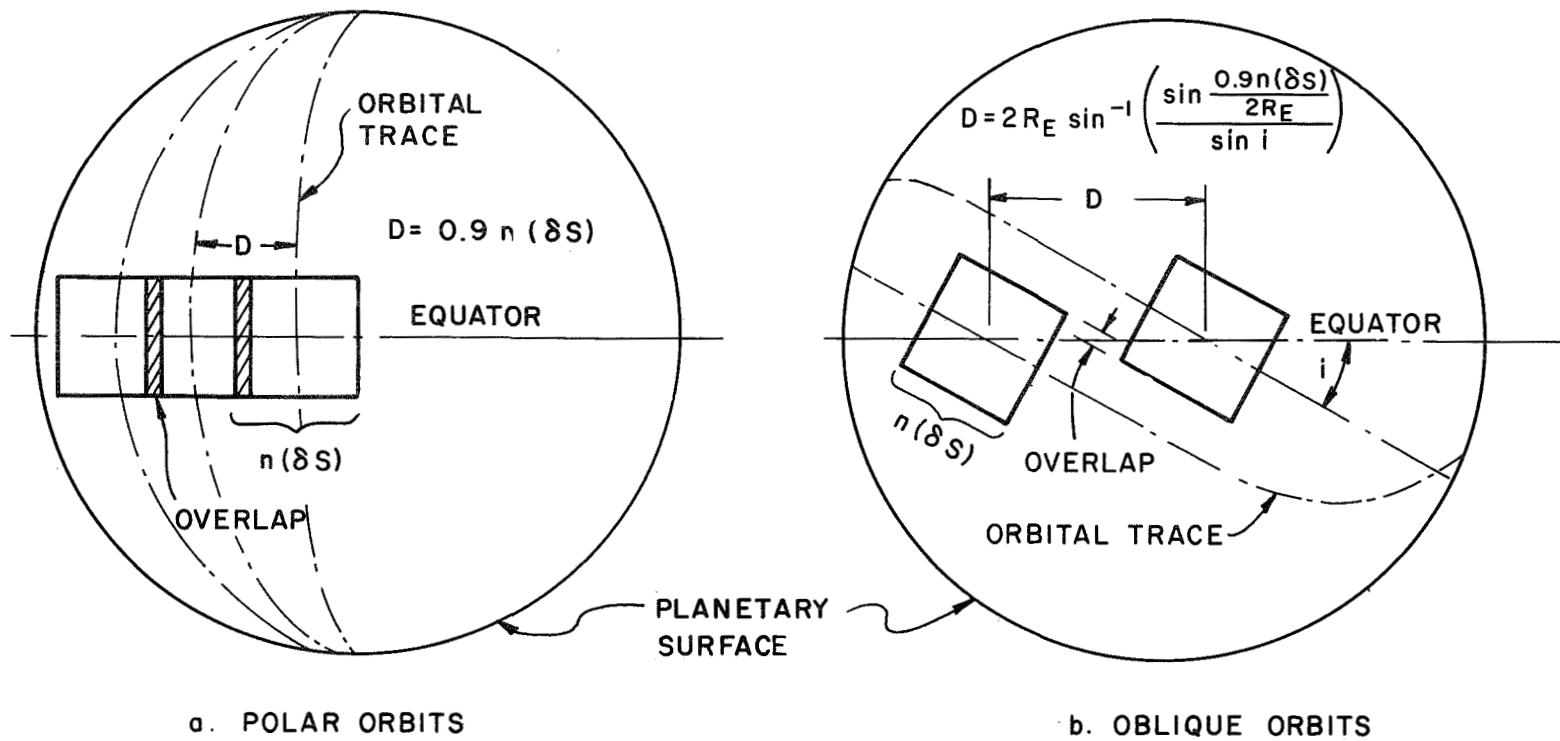orbital inclination. Figure 12b depicts the increase in spacing

Figure 12.- Image frame constraints on orbit spacing

associated with a decrease in angle of inclination. The associated planar approximation leads to

$$D' = \frac{0.9 \ n(\delta s)}{\sin i} \qquad (20)$$

The advantage of Eq. (20) over Eq. (19) is that it no longer contains the planetary radius and so is generally applicable to all planets. The errors in using this approximation are shown by the curves of Figure 13. It appears then that this approximation is justified within the limited scope of the present study. In place of Eq. (18) one obtains

$$N = \left[\frac{C_E}{D'}\right]' = \left[\frac{C_E \ \sin i}{0.9 \ n(\delta s)}\right]' \qquad (21)$$

for orbits of any inclination.

The orbital period of the spacecraft, P, is given by

$$P = 2\pi \sqrt{a^3/\mu} \qquad (22)$$

where a = semi-major axis and $\mu = m_i G$ with m_i the mass of the ith planet and G the universal gravitational constant. If one applies the constraint that complete coverage is to be obtained with a minimum number of orbits, then the total minimum time for the mapping operation is NP. Total coverage implies that the N + 1th orbit must retrace the 1st orbit. Thus, an integer number of rotations of the planet must take place during the time NP. If the siderial period of rotation of the planet is T, then for various integer values of a multiplying factor K (not the same as the overlap fraction) the following results

$$NP = KT \qquad (23)$$

Transposing terms

$$N = K \frac{T}{P} \qquad K = 1, \ 2, \ \ldots \qquad (24)$$

N and T are fixed numbers so that the orbital period of the spacecraft (and hence "a") must assume discrete or quantized values dependent upon the quantum number K.

Not all values of K are permitted, however. If N is divisible by any factor of K (except 1) periodicities in the mapping coverage will result which will prevent the entire surface from being mapped.
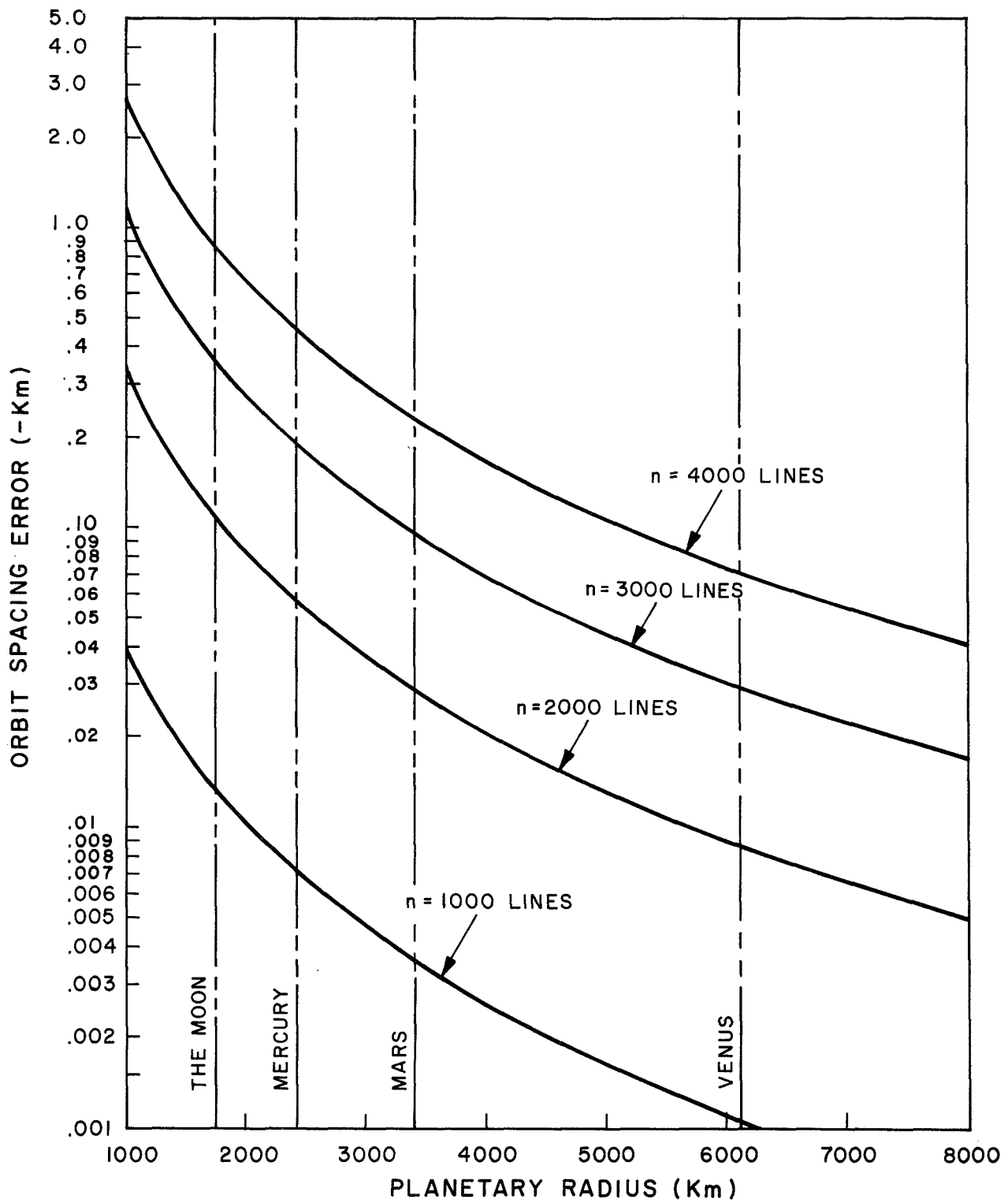
Figure 13.- Orbit spacing approximation errors
inclination — 30 degrees
mapping scale — 1:10^6

If N is prime, all values of K are permissable. The integer K then also is the number of diurnal periods required for complete mapping coverage. The forbidden levels may also be specified in terms of the fraction N/K. All values of K are permitted for which the fraction N/K is irreducible. It is still highly desirable that N be prime so that all values of K are permitted. Tables V, VI, and VII list the values of N calculated for the mapping parameters of Table II and the planets of Table III for orbital inclinations of 90 degrees, 60 degrees, and 30 degrees, respectively. The nearest prime numbers to these values of N are given in the parentheses.

Sets of permitted orbital levels have been generated for the following cases:

Body	Scale	Inclination	Table
Moon	$1:10^6$	90°	VIII
Moon	$1:10^6$	30°	IX
Mars	$1:10^6$	90°	X
Mars	$1:10^6$	30°	XI
Mars	$1:5 \times 10^6$	90°	XII
Mars	$1:5 \times 10^6$	30°	XIII
Jupiter	$1:5 \times 10^6$	90°	XIV

The values of K employed and corresponding orbital altitudes, semi-major axes, and orbital periods are presented in the preceeding tables. The orbital-levels data obtained lead to interesting and somewhat unexpected results.

Contrary to intuitive predictions, high-resolution (greater than 1000 lines) imaging systems prove of little value for lunar cartography at a mapping scale of $1:10^6$. The long diurnal period results in little surface movement of the trace of the inertially fixed orbit. Tables VIII and IX indicate that very high orbits, and hence large spacecraft orbital periods, are required to take advantage of any large number of resolution elements. The altitudes of such orbits must be measured in thousands of kilometers. If these orbits were to be employed, the associated attitude problems (reference, stabilization, and pointing) would become extremely difficult to solve. In addition, at such altitudes, orbital perturbations due to the Earth, the Sun, and the nearby planets become significant. Mars and Jupiter, the other two planetary bodies studied in detail, do not present this problem due to their relatively short diurnal periods.

TABLE V.   VALUES OF N
90 DEG INCLINATION ORBIT

Scale	n	Moon	Mercury	Venus	Mars	Jupiter	Saturn
$1:10^6$	500	486 (487)	676 (677)	1704 (1709)	948 (947)	19936	16867
	1000	243 (241)	338 (337)	857 (857)	474 (479)	9968	8434
	2000	122 (127)	169 (167)	429 (431)	237 (239)	4984	4217
	3000	81 (83)	113 (113)	284 (283)	158 (157)	3323	2812
	4000	61 (61)	85 (83,89)	215 (223)	119 (127)	2492	2109
$1:5 \times 10^6$	500	97 (97)	136 (137)	341 (347)	190 (191)	3988 (3989)	3374
	1000	49 (53)	68 (67)	171 (173)	95 (97)	1999 (1999)	1687 (1693)
	2000	25 (29)	34 (37)	86 (89)	48 (47)	1000 (997)	844 (839)
	3000	17 (17)	23 (23)	57 (59)	32 (31)	665 (661)	563 (563)
	4000	13 (13)	17 (17)	43 (43)	24 (23)	500 (499)	422 (421)

TABLE VI.   VALUES OF N
60 DEG INCLINATION ORBIT

Scale	n	Moon	Mercury	Venus	Mars	Jupiter	Saturn
$1:10^6$	500	421 (421)	586 (587)	1476 (1481)	821 (821)	17265	14608
	1000	211 (211)	293 (293)	738 (739)	411 (409)	8633	7304
	2000	105 (107)	147 (149)	369 (367)	206 (211)	4316	3652
	3000	70 (71)	98 (97)	246 (251)	137 (137)	2878	2435
	4000	53 (53)	74 (79)	185 (191)	103 (103)	2158	1826
$1:5 \times 10^6$	500	84 (89)	117 (113)	295 (293)	165 (167)	3453	2922
	1000	42 (43)	59 (59)	148 (149)	83 (83)	1727 (1723)	1461 (1459)
	2000	21 (23)	30 (31)	74 (79)	41 (41)	864 (863)	731 (733)
	3000	14 (17)	20 (23)	50 (53)	28 (29)	576 (577)	487 (487)
	4000	11 (11)	15 (17)	37 (37)	21 (23)	432 (433)	366 (367)

TABLE VII.   VALUES OF N
30 DEG INCLINATION ORBIT

Scale	n	Moon	Mercury	Venus	Mars	Jupiter	Saturn
$1:10^6$	500	243 (241)	338 (337)	852 (853)	474 (479)	9968	8434
	1000	122 (127)	169 (167)	426 (431)	237 (239)	4984	4217
	2000	61 (61)	85 (89)	213 (211)	119 (127)	2492	2109
	3000	41 (41)	57 (59)	142 (139)	79 (79)	1662 (1663)	1406 (1409)
	4000	31 (31)	43 (43)	107 (107)	60 (61)	1246 (1249)	1055 (1051)
$1:5 \times 10^6$	500	49 (53)	68 (67)	171 (173)	95 (97)	1994 (1993)	1687 (1693)
	1000	25 (29)	34 (37)	86 (89)	48 (47)	997 (997)	844 (839)
	2000	13 (13)	17 (17)	43 (43)	24 (29)	499 (499)	422 (421)
	3000	9 (11)	12 (13)	29 (29)	16 (17)	333 (331)	282 (283)
	4000	7 (7)	9 (11)	22 (23)	12 (13)	250 (251)	211 (211)

The number of Earth days required to map Mars corresponds almost exactly to the number K because the diurnal periods of both planets nearly coincide. A sizeable number of orbital levels are available for 1:10^6 scale mapping (Tables X and XI). Extremely fine resolution is not required since it will only take about 20 days for complete coverage from polar orbit for 2000 resolution elements per image frame side (n = 2000). Mapping from an orbit of 30 degrees inclination will take but half as long, all other parameters remaining fixed. For 1:5 x 10^6 scale mapping of Mars (Tables XII and XIII), the lower resolutions should prove more desirable than the middle to high values of n because they permit sufficient orbital levels to ease the orbital shaping problem.

Mapping Jupiter from polar orbit at a scale of 1:5 x 10^6 (Table XIV) will be a time-consumming operation even with the highest resolution system. The time required for complete coverage is, approximately, 0.4K Earth days. The following list indicates the time needed to yield one set of images of the entire planet for each of the values of n employed:

n	Time (Days)
500	500
1000	250
2000	130
3000	85
4000	65

The longer times can cause several problems in term of mission operation. Reliability is a problem for any mission of several years duration. Communications and data relay are seriously affected if, during a single mapping pass, one-half of an Earth year or more passes. Now one is faced with changes in path length of up to 2 astronomical units (AU); that is, the entire diameter of the Earth's orbit. Over long periods of time, perturbations of the spacecrafts orbit will probably induce large angles of precession. The orbit will not be able to retain a desired orientation with respect to the sun line and planet without a series of corrective actions. Lastly, Jupiter's appearance will be changing throughout the mapping operation. It is the atmosphere and not the surface which is being mapped in this case. Thus if the time for complete coverage is great, there is a good chance that imagery, adjacent in space but not in time, will not connect from one frame to another. The mapped surface will have changed in the time interval between adjacent orbital passes.

TABLE VIII. LUNAR ORBITAL LEVELS,
1:10^6 SCALE MAPPING
90 DEG INCLINATION

Diurnal Period = 39,343.68 min
Equatorial Radius 1,738 km

n = 500	N = 487		
K	a (km)	h (km)	P (min)
2	2,269	531	161.57
3	2,973	1,235	242.36
4	3,601	1,863	323.15
5	4,179	2,441	403.94
6	4,719	2,981	484.73
7	5,230	3,492	565.51
8	5,716	3,978	646.30

n = 1000	N = 241		
K	a (km)	h (km)	P (min)
1	2,284	546	163.25
2	3,626	1,888	326.50
3	4,751	3,031	489.76
4	5,756	4,018	653.01

.n = 2000	N = 127		
K	a (km)	h (km)	P (min)
1	3,501	1,763	309.79
2	5,558	3,820	619.59

n = 3000	N = 83		
K	a (km)	h (km)	P (min)
1	4,649	2,911	474.02

n = 4000	N = 61		
K	a (km)	h (km)	P (min)
1	5,709	3,971	644.98

TABLE IX. LUNAR ORBITAL LEVELS,
1:10^6 SCALE MAPPING
30 DEG INCLINATION

Diurnal Period = 39,343.68 min
Equatorial Radius = 1,738 km

n = 500	N = 241		
K	a (km)	h (km)	P (min)
1	2,284	546	163.25
2	3,626	1,888	326.50
3	4,751	3,031	489.76
4	5,756	4,018	653.01

n = 1000	N = 127		
K	a (km)	h (km)	P (min)
1	3,501	1,763	309.79
2	5,558	3,820	619.59

n = 2000	N = 61		
K	a (km)	h (km)	P (min)
1	5,709	3,971	644.98

n = 3000			N = 41
K	a (km)	h (km)	P (min)
1	7,441	5,703	959.60

n = 4000			N = 31
K	a (km)	h (km)	P (min)
1	8,963	7,225	1269.15

TABLE X. MARTIAN ORBITAL LEVELS,
$1:10^6$ SCALE MAPPING
90 DEG INCLINATION

Diurnal Period = 1,477.38 min
Equatorial Radius = 3,395 km

n = 500			N = 947
K	a (km)	h (km)	P (min)
65	3,427	32	101.40
66	3,462	67	102.96
67	3,497	102	104.52
68	3,532	137	106.08
69	3,566	171	107.64
70	3,601	206	109.20
71	3,635	240	110.76
72	3,669	274	112.32
73	3,703	308	113.88
74	3,737	342	115.44
75	3,771	376	117.00
76	3,804	409	118.56
77	3,837	442	120.12
78	3,870	475	121.68
79	3,903	508	123.25
80	3,936	541	124.81
81	3,969	574	126.37
82	4,002	607	127.93

83	4,034	639	129.49
84	4,066	671	131.05
85	4,098	703	132.61
86	4,130	735	134.16
87	4,162	767	135.73
88	4,194	799	137.29
89	4,226	831	138.85
90	4,258	863	140.41
91	4,289	894	141.97
92	4,321	926	143.53
93	4,352	957	145.09
94	4,383	988	146.65

n = 1000			N = 947
K	a (km)	h (km)	P (min)
34	3,505	101	104.87
35	3,573	178	107.95
36	3,641	246	111.03
37	3,708	313	114.12
38	3,775	380	117.20
39	3,840	445	120.29
40	3,906	511	123.37
41	3,971	576	126.46
42	4,035	640	129.54
43	4,099	704	132.62
44	4,162	767	135.71
45	4,225	830	138.79
46	4,287	892	141.88
47	4,349	954	144.96

n = 2000		N = 239	
K	a (km)	h (km)	P (min)
17	3,510	115	105.09
18	3,646	251	111.27
19	3,780	385	117.45
20	3,911	516	123.63
21	4,041	646	129.81
22	4,168	773	135.99
23	4,293	898	142.17

n = 3000		N = 157	
K	a (km)	h (km)	P (min)
11	3,474	79	103.51
12	3,682	287	112.92
13	3,884	489	122.33
14	4,081	686	131.74
15	4,273	876	141.15

n = 4000		N = 119	
K	a (km)	h (km)	P (min)
9	3,656	261	111.73
10	3,922	527	124.15
11	4,180	785	135.56

38	3,775	380	117.20
39	3,840	445	120.29
40	3,906	511	123.37
41	3,971	576	126.46
42	4,035	640	129.54
43	4,099	740	132.62
44	4,162	767	135.71
45	4,225	830	138.79
46	4,287	892	141.88
47	4,349	954	144.96
48	4,411	1,016	148.05

n = 1000		N = 239	
K	a (km)	h (km)	P (min)
17	3,510	115	105.09
18	3,646	251	111.27
19	3,780	385	117.45
20	3,911	516	123.63
21	4,041	646	129.81
22	4,168	773	135.99
23	4,293	898	142.17
24	4,417	1,022	148.36

TABLE XI. MARTIAN ORBITAL LEVELS,
1:10^6 SCALE MAPPING
30 DEG INCLINATION

Diurnal Period = 1,477.38 min
Equatorial Radius = 3,395 km

n = 500		N = 479	
K	a (km)	h (km)	P (min)
33	3,436	41	101.78
34	3,505	110	104.87
35	3,573	178	107.95
36	3,641	246	111.03
37	3,708	313	114.12

n = 2000		N = 119	
K	a (km)	h (km)	P (min)
9	3,656	261	111.73
10	3,922	527	124.15
11	4,180	785	136.56
12	4,429	1,034	148.98

n = 3000		N = 79	
K	a (km)	h (km)	P (min)
6	3,667	272	112.21
7	4,063	668	130.91
8	4,441	1,046	149.61

n = 4000		N = 61	
K	a(km)	h(km)	P(min)
5	3,858	463	121.10
6	4,357	962	145.32
7	4,828	1,433	169.55

TABLE XII. MARTIAN ORBITAL LEVELS,
1:5 x 10⁶ SCALE MAPPING
90 DEG INCLINATION

Diurnal Period = 1,477.38 min
Equatorial Radius = 3,395 km

n = 500		N = 191	
K	a(km)	h(km)	P(min)
13	3,408	13	100.55
14	3,581	186	108.29
15	3,749	354	116.02
16	3,914	519	123.76
17	4,075	680	131.49
18	4,234	839	139.23
19	4,389	994	146.96

n = 1000		N = 95	
K	a(km)	h(km)	P(min)
7	3,593	198	108.86
8	3,928	533	124.41
9	4,249	854	139.96
10	forbidden		
11	4,857	1,462	171.07

n = 2000		N = 47	
K	a(km)	h(km)	P(min)
4	3,956	561	125.73
5	4,590	1,195	157.17
6	5,183	1,783	188.60

n = 3000		N = 31	
K	a(km)	h(km)	P(min)
3	4,309	914	142.97
4	5,220	1,825	190.63

n = 4000		N = 25	
K	a(km)	h(km)	P(min)
2	3,796	401	118.19
3	4,974	1,579	177.29

TABLE XIII. MARTIAN ORBITAL LEVELS,
1:5 x 10⁶ SCALE MAPPING
30 DEG INCLINATION

Diurnal Period = 1,477.38 min
Equatorial Radius = 3,395 km

n = 500		N = 97	
K	a(km)	h(km)	P(min)
7	3,544	149	106.62
8	3,874	479	121.85
9	4,190	795	137.08
10	4,495	1,100	152.31

n = 1000		N = 47	
K	a(km)	h(km)	P(min)
4	3,956	561	125.73
5	4,590	1,195	157.17
6	5,183	1,788	188.60

n = 2000		N = 25	
K	a(km)	h(km)	P(min)
2	3,796	401	118.19
3	4,974	1,579	177.29

n = 3000		N = 17	
K	a(km)	h(km)	P(min)
2	4,909	1,514	173.81

n = 4000		N = 499	
K	a(km)	h(km)	P(min)
152	72,038	650	179.87
153	72,353	966	181.06
154	72,668	1,281	182.24
155	72,983	1,595	183.42

n = 4000		N = 13	
K	a (km)	h (km)	P (min)
1	3,698	303	113.64

1237	72,901	1,514	183.12
1238	72,941	1,553	183.26
1239	72,980	1,592	183.41

TABLE XIV. JOVIAN ORBITAL LEVELS,
1:5 x 10^6 SCALE MAPPING
90 DEG INCLINATION

Diurnal Period = 590.50 min
Equatorial Radius = 71,387 km

n = 500		N = 3989	
K	a (km)	h (km)	P (min)
1214	71,995	607	179.71
1215	72,034	647	179.86
1216	72,074	686	180.01
1217	72,113	726	180.16
1218	72,153	765	180.30
1219	72,192	805	180.45
1220	72,232	844	180.60
1221	72,271	884	180.75
1222	72,311	923	180.90
1223	72,350	963	181.04
1224	72,390	1,002	181.19
1225	72,429	1,041	181.34
1226	72,468	1,081	181.49
1227	72,508	1,120	181.64
1228	72,547	1,160	181.78
1229	72,587	1,199	181.93
1230	72,626	1,238	182.08
1231	72,665	1,278	182.23
1232	72,705	1,317	182.38
1233	72,744	1,356	182.52
1234	72,783	1,396	182.67
1235	72,823	1,435	182.82
1236	72,862	1,474	182.97

n = 1000		N = 1999	
K	a (km)	h (km)	P (min)
609	72,045	657	179.90
610	72,123	736	180.19
611	72,202	815	180.49
612	72,281	893	180.78
613	72,360	972	181.08
614	72,438	1,051	181.37
615	72,517	1,130	181.67
616	72,596	1,208	181.96
617	72,674	1,287	182.26
618	72,753	1,365	182.56
619	72,831	1,444	182.85
620	72,910	1,522	183.15

n = 2000		N = 997	
K	a (km)	h (km)	P (min)
304	72,086	699	180.05
305	72,224	857	180.64
306	72,402	1,015	181.24
307	72,560	1,172	181.83
308	72,717	1,330	182.42
309	72,875	1,487	183.01

n = 3000		N = 661	
K	a (km)	h (km)	P (min)
202	72,193	806	180.46
203	72,432	1,044	181.35
204	72,669	1,282	182.24
205	72,906	1,519	183.14

GUIDANCE AND CONTROL REQUIREMENTS

In support of the cartographic payload, an onboard guidance and control subsystem may be required to perform the following operations:

Group I

 a. Boost guidance (from Earth) and attitude stabilization.
 b. Injection guidance from parking orbit
 c. Mid-course attitude and thrust control
 d. Deboost into planetary orbit
 e. Planetary orbit trim
 f. Orbital navigation
 g. Orbital transfer and correction
 h. Spacecraft stabilization

Group II

 i. Pointing of imaging subsystem
 j. Precise attitude reference
 k. Pointing of communication subsystem
 l. Image motion compensation
 m. Exposure timing and control
 n. Image annotation

Group I items pertain to the spacecraft's normal G&C operations while those in Group II are required specifically for the operation of the onboard imaging system. Although only Group II requirements are derived in the following sections, G&C systems capable of both Group I and Group II operations were considered as well as those only for the latter. In the following section a representative example of each is presented. These typical (not necessarily optimum) configurations are then used to aid in the generation of specific guidance and control requirements.

The Guidance and Control Subsystem

At present, techniques exist for processing appropriate pairs of skew-oriented photographic images so as to yield orthographic and contour map representations of the imaged areas. Such techniques, however, are time consuming requiring cross-correlation of both images at increments of displacement corresponding to the smallest resolution element in either image. In addition, they yield no absolute level plane (geodetic reference figure) or position reference. The data to be obtained from any complete planetary survey would (in most instances) overload our capability to process the primary images in the above manner. Thus, it has been assumed that the primary objectives of the systems proposed and discussed in this study are:

 a. To supply an absolute reference for the resulting maps to the accuracy specified in Table I, and

b. To provide sufficient reference information for each image so that the entire map generation process can be reduced to a completely automatic explicit process; so that correlation or similar scan and evaluation techniques prove unnecessary.

It is in light of these objectives that the two basically different G&C systems have been postulated as already noted. One will only meet Group II operational requirements (Figure 14) lacking as it does any inertial measurement (or reference) unit. Image attitude reference is obtained through continuous use of the various celestial trackers. The other (Figure 15), in addition to providing a combined
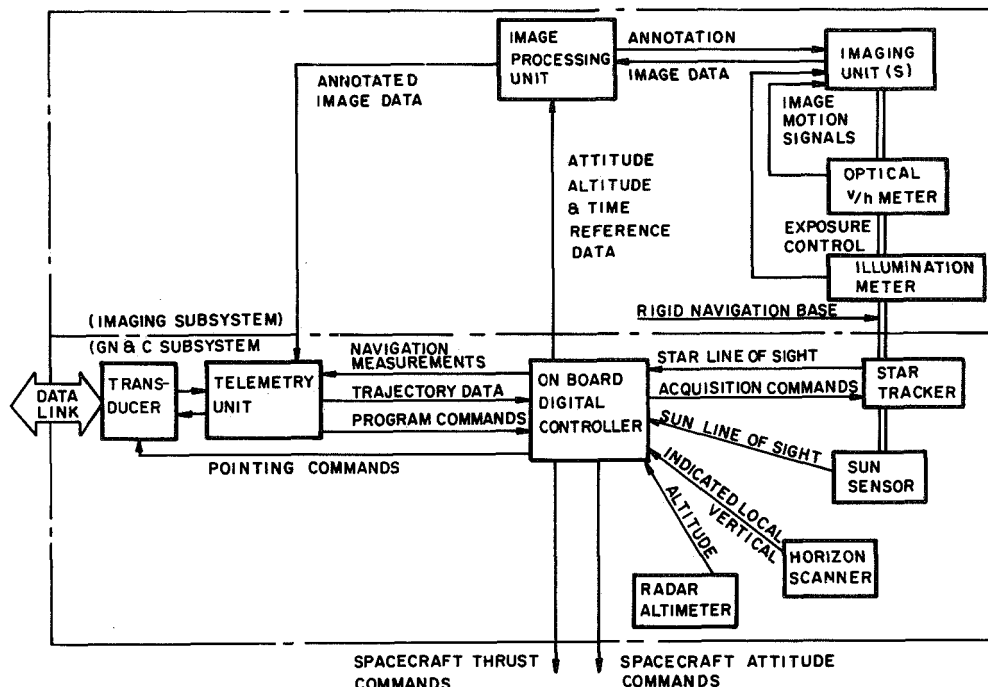
Figure 14.- Cartographic-support-limited guidance, navigation and control system schematic

Group I & II capability, through incorporation of a larger digital computer and an inertial measurement unit, also provides a smooth inertially derived attitude reference which needs to be updated only periodically by the various celestial trackers.

In both systems, all onboard sensors and optical elements are maintained in alignment through mounting to a common rigid navigation base. In both systems, basic navigation is performed by the DSIF. Precise determination of the spacecraft's position in orbit need not be made, however, on a real-time basis. If each image is adequately annotated (time, attitude, etc.) post-flight trajectory processing would prove satisfactory. In the more complicated system (particularly because it is configured so as to guide and control the entire

space vehicle from boost through the cartographic operation), a wider
range of onboard functions can be provided than by the system without
a complete inertial reference unit. Figure 14 shows image motion
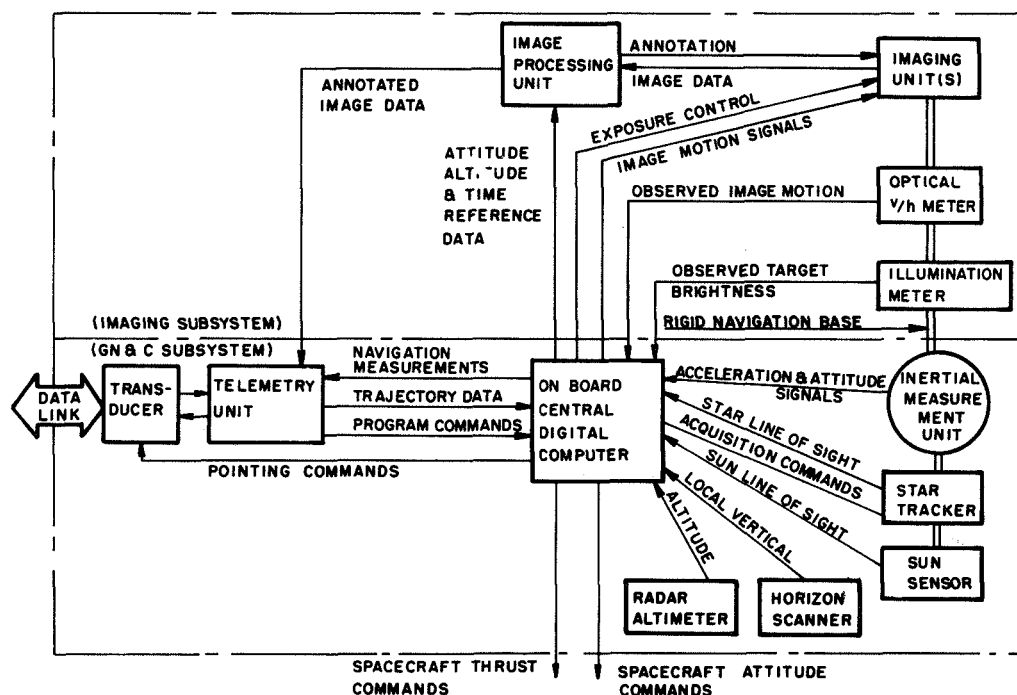
Figure 15.- Overall-mission-capability guidance,
navigation, and control system

and image exposure controlled directly by means of the signals gen-
erated by special onboard optical sensors. In Figure 15, options are
provided for completely analytical or mixed analytical-optical or
completely optical approachs.

An important difference between the two G&C systems is associated
with the use, or lack of use, of a gyroscopically derived attitude
reference. When the inertial measurement unit is present, the accuracy
required of the celestial trackers in only on the order of that re-
quired to meet the positional accuracy specifications of Table I.
Completely automatic processing of the images is still possible be-
cause (except for unusually high gyro drift rates) the change in
attitude between corresponding image pairs will be small compared to
a single resolution element. For a system without an inertial attitude
reference, either the accuracy of the celestial trackers must be 6
times as great as that for the more complicated system (since the
dimension of an object resolution element is but 1/6 of that of the
specified positional accuracy) or the map generation process must be
increased in complication. In the latter instance, either some form
of image correlation must again be employed or man must be introduced
into the loop for the purpose of identifying common reference points
in corresponding images. In either case, guidance and control accuracy
requirements are directly related to cartographic requirements.

32

Position and Attitude in Orbit

The positional uncertainty of image location in the object plane is a combined function of the orbital position and attitude reference uncertainties of the spacecraft (Figure 16). If it is assumed that the altitude of the spacecraft above the planetary surface is small compared with the radius of this surface and that the attitude reference uncertainty is small, the rss value of the error in image location (ε_{il}) is given by

$$\varepsilon_{il} = \left[(\varepsilon_{orb. \ pos.})^2 + (\varepsilon_{att.} \times h)^2 \right]^{1/2} \qquad (25)$$
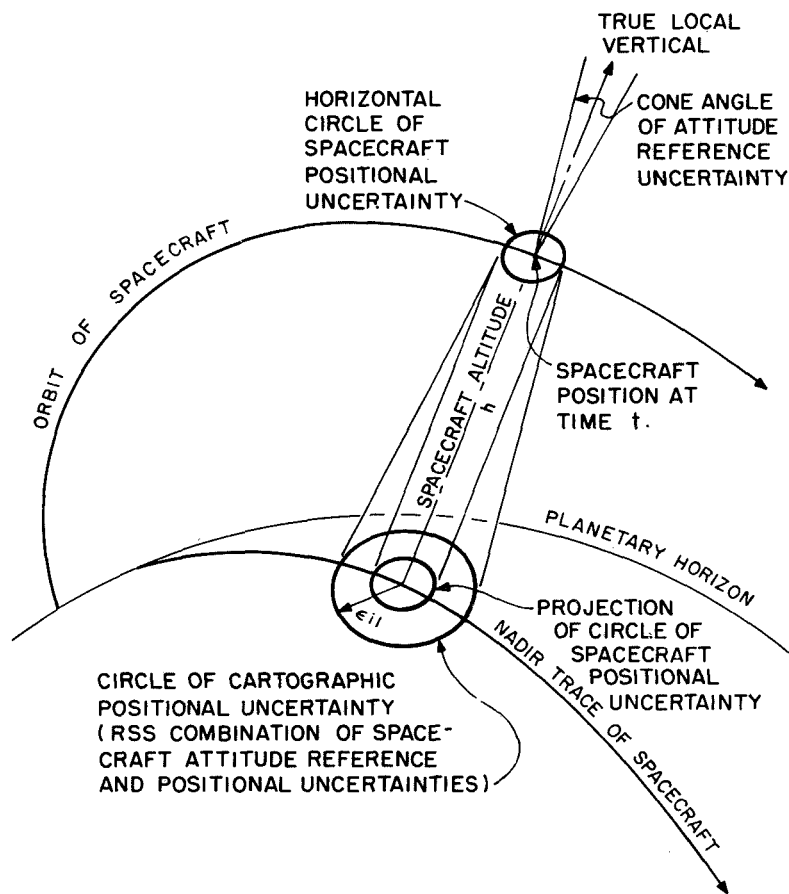
Figure 16.- Geometry of image positional uncertainty

A value of ε_{il} is required for each mapping scale in order to solve parametrically for the terms on the right hand side of Eq. (25). Now, the entire surface area of the planet will be imaged twice

(ignoring overlap) so that an accuracy improvement on the order of $\sqrt{2}$ for any position determination should be expected over that of any single determination. Thus, using Table I, ε_{il} takes on values:

Scale	ε_{il} (meters)
$1:10^6$	423
$1:5 \times 10^6$	2120

Assuming a spherical distribution for spacecraft positional uncertainty, Eq. (25) has been represented graphically by Figures 17 and 18 for the $1:10^6$ and $1:5 \times 10^6$ scales, respectively. For the former, curves were generated for the values 100, 200, 300, and 400 meters orbital position uncertainty; for the latter, values of 400, 800, 1200, 1600 and 2000 meters were employed. The resulting altitude dependence points out the value in achieving as low an orbit as possible for a particular mapping situation.
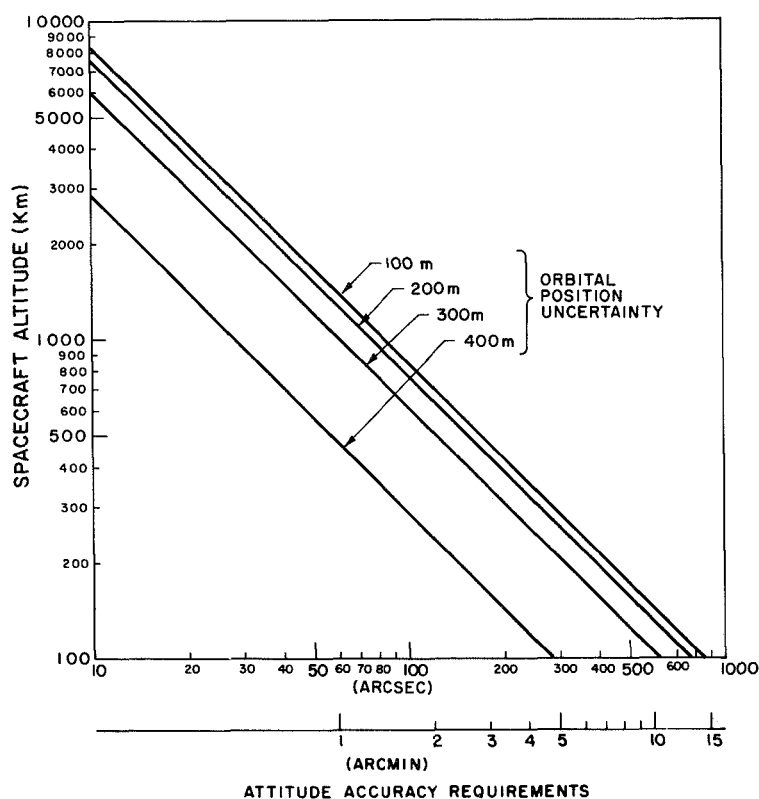
Figure 17.- Required reference attitude accuracy $1:10^6$ scale mapping
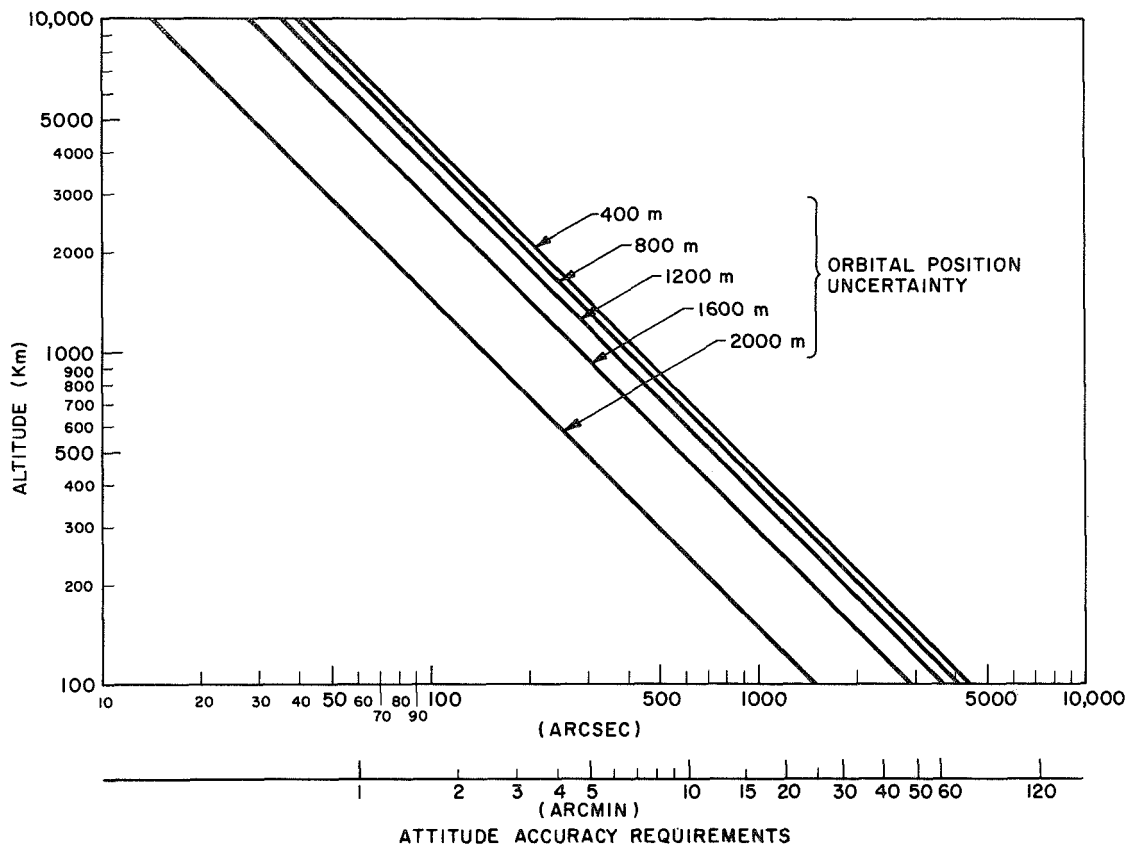
Figure 18.- Required reference attitude accuracy
1:5 x 10^6 scale mapping

If an onboard G&C system of the class represented by Figure 14 is to be employed, then Figure 17 or 18 may be used directly to obtain the limiting accuracies for the onboard optical sensors. If a system of the class represented by Figure 15 is selected (with all the resultant simplifications in the image processing operation), then the effect of gyro drift between periods of attitude update must be considered. The rss value of $\varepsilon_{attitude}$ is given by

$$\varepsilon_{attitude} = \left[(\delta\phi_{init})^2 + (t \times d_{gyro})^2 \right]^{1/2} \tag{26}$$

where $\delta\phi_{init}$ = initial angular misalignment (tracker accuracy)

   t = time between updates

d_{gyro} = 3 axis combined gyro drift rate

For the graphical representation of Eq. (26), discrete values of $\delta\phi_{init}$ and d_{gyro} were chosen which correspond to actual classes of

35

equipment performances. Thus, values of .001-deg/hr, .01-deg/hr and .1-deg/hr were used for gyro drift rate and of 10 arcseconds, 20 arcseconds, 1 arcminute, 3 arcminutes, 6 arcminutes, and 10 arc- minutes for the accuracies of the celestial trackers to be used for initial attitude alignment or update. Attitude accuracy is then shown as a function of time between update by Figure 19.
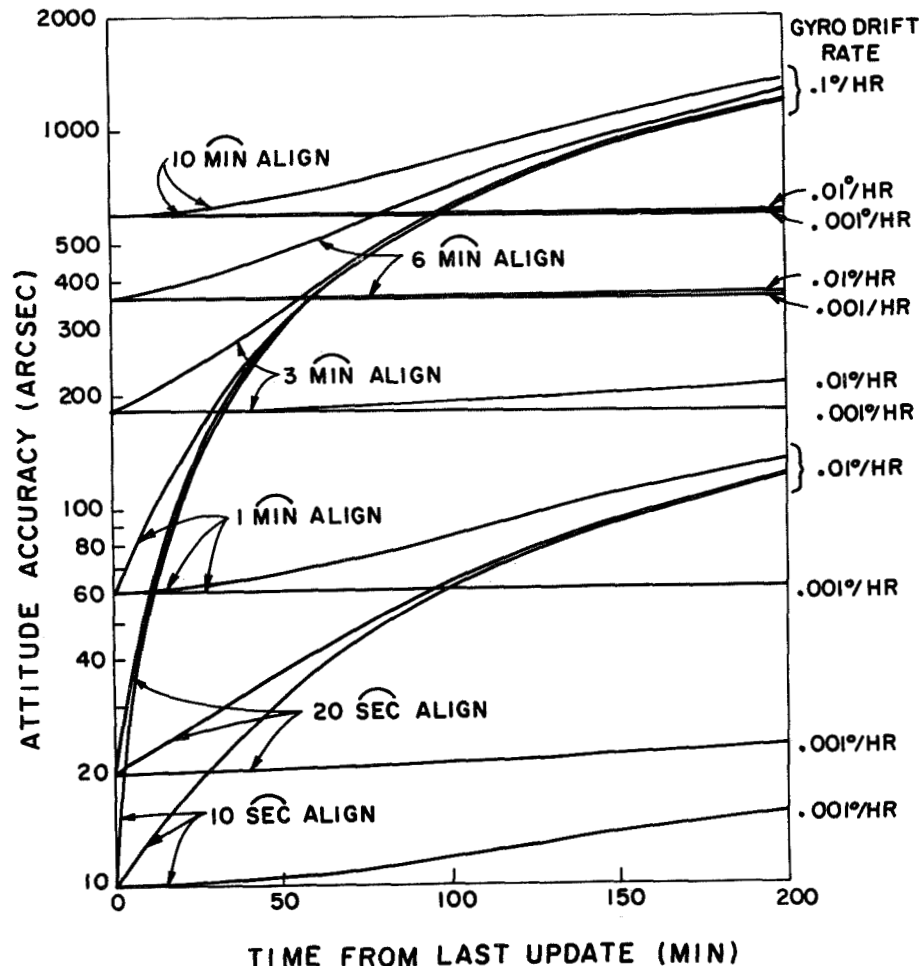

Figure 19.- Propagation of attitude reference errors
Camera Pointing Accuracy

The problem of position and attitude reference is described in the preceeding section. The problem of camera pointing accuracy on the other hand is not nearly so severe as may have been expected. Image overlap (in part) is provided so as to absorb the various image field displacement errors due to camera pointing errors, orbital navigation (and hence orbital period) errors and exposure timing errors. Here, camera pointing errors are examined.

Image field rotation is directly proportional to camera yaw error δ(yaw) (rotation about the local vertical). If the maximum image

36

displacement error due to yaw is limited to one-fourth of the image overlap (a value of 10 percent image overlap is used throughout this report) then it can be shown that,

$$\delta \text{ (yaw)} = \pm 2° \text{ 48'} \tag{27}$$

To obtain the limits on δ (yaw) for other fractions of the image overlap, direct proportionalities should be applied.

The effects of roll and pitch (or cross local vertical) errors, on the other hand, are altitude dependent. (Figure 20) has been prepared for both the nadir pointing and oblique pointing cases allowing a maximum image displacement in either direction (down range or cross range) of one-half of the 10 percent overlap (or 5 percent of the entire image area). By use of field of view rather than altitude as the independent variable, all the appropriate mapping parameters (scale, resolution number, altitude) are covered by the two curves of Figure 20. This approach is then consistent with Figures 8 through 11.
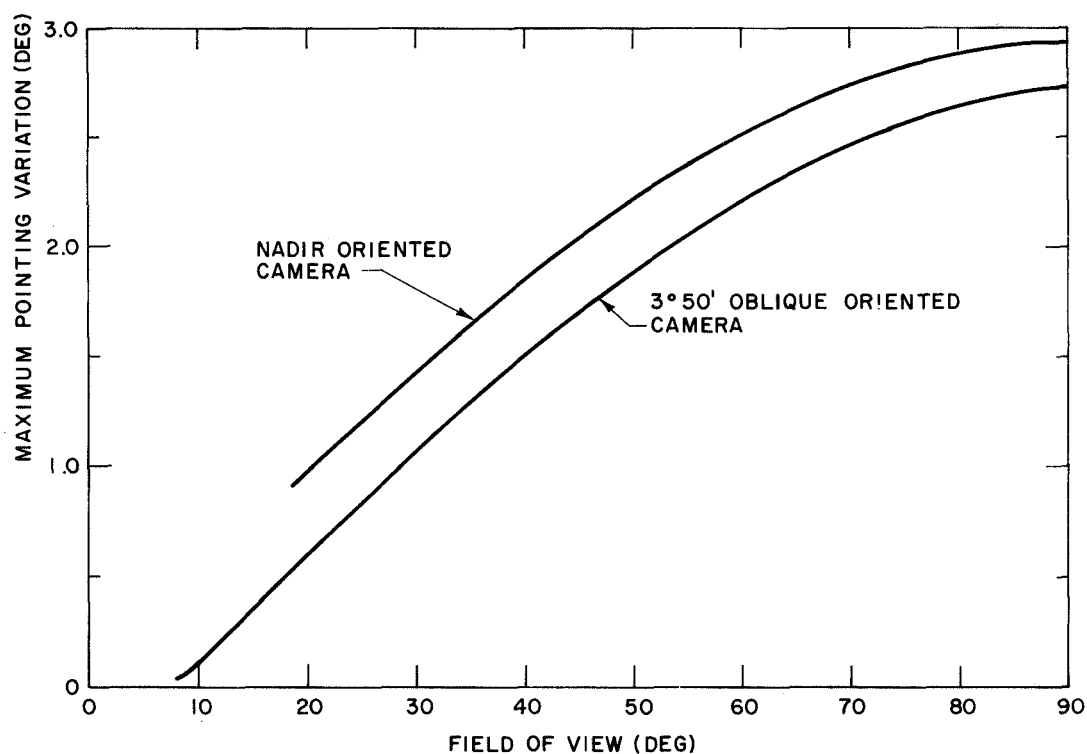
Figure 20.- Camera pointing accuracy requirements in roll and pitch (5% maximum image displacements)

Image Motion Compensation

To meet given resolution requirements, the product of image motion rate and length of the maximum image exposure time should be some moderately small fraction of the least resolution element. Before developing instrumentation to provide required image motion compensation, it is necessary to determine the sources and extent of this motion. Here, three such sources are identified and quantitative results are generated (as applicable) for the Moon, Mars, and Jupiter. The three sources are:

1. Angular rate of spacecraft rotation about each of its three axes (roll, pitch, yaw).

2. Orbital velocity of the spacecraft above the surface of the planet (north-south motion for a polar orbit).

3. Tangential velocity at the planet's surface due to diurnal rotation (function of latitude).

A value of 0.01 deg/sec has been used as representative of the angular rate of spacecraft rotation. For other values, the image motion rate data may be scaled accordingly. A yaw rate produces maximum image motion at the edge of the field. A higher resolution number (n) means a larger image field. Thus image motion due to a rate of rotation about the yaw axis (Figure 21) is a function of the number of resolution elements and the mapping scale. (Image motion is presented in terms of apparent object plane motion throughout this development.) Image motion due to pitch (or roll) motion, on the other hand, is only a function of altitude for small total angular displacements about the desired pointing direction (Figure 22).
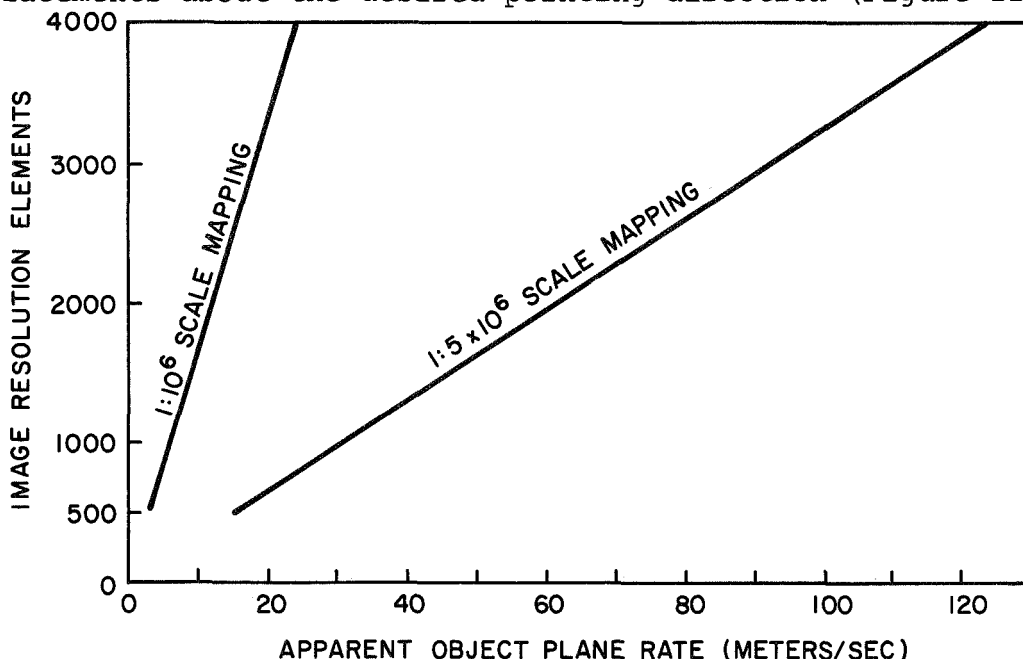

Figure 21.- Image motion at edge of field due to 0.01°/sec yaw rate
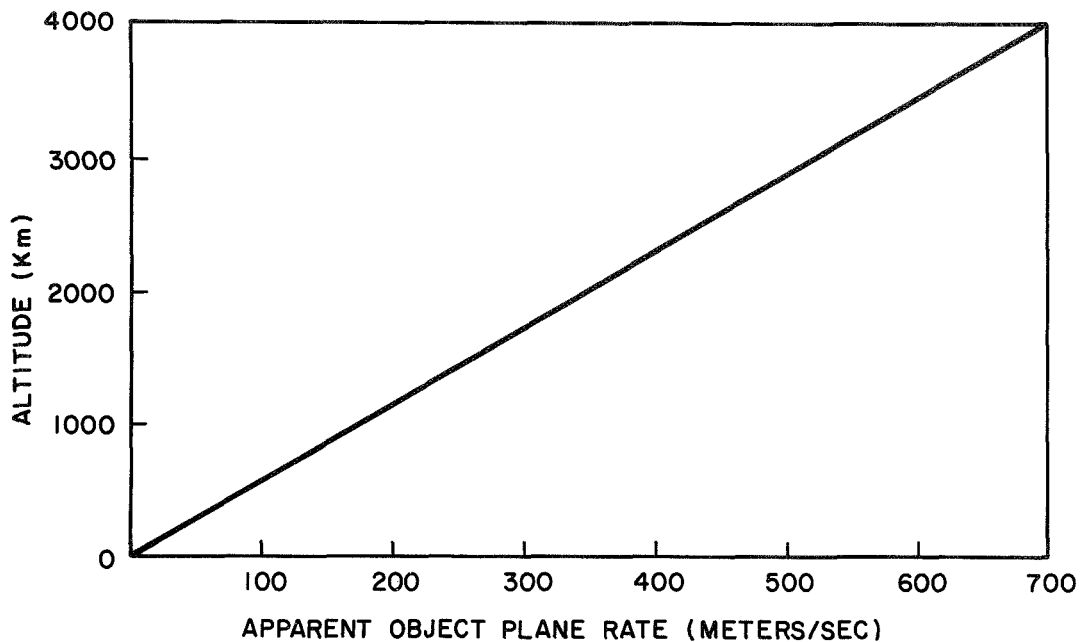
Figure 22.- Image motion due to pitch (or roll)
rate of 0.01°/sec

The tangential velocity of a spacecraft due to its orbital motion
is a function of both the specific planet and the distance of the
spacecraft from its center. (For purposes of simplification, it has
been assumed that all spacecraft orbits are essentially circular).
The curves of (Figure 23) give values for this source of image motion
as a function of altitude for the Moon, Mars, and Jupiter. This is
the major component of image motion.

The diurnal rotation of the Moon produces negligible image
motion (Figure 24a) having a maximum value at its equator of less
than 5 m/sec. Mars, on the other hand, produces moderate values of
this same quantity having a rate of about 240 m/sec at its equator
(Figure 24b). Jupiter with its large radius and short diurnal period
has equatorial rates of over 12,000 m/sec (Figure 24c). Such rates
are on the order of magnitude of those due to spacecraft orbital
motion (Figure 23).

Specific Applications

To illustrate the use of the tables, graphs, and numerical
results presented in this paper, a specific mission has been selected
for the generation of guidance and control requirements. Let us
suppose that it is desired to map Mars at a scale of $1:10^6$ from polar
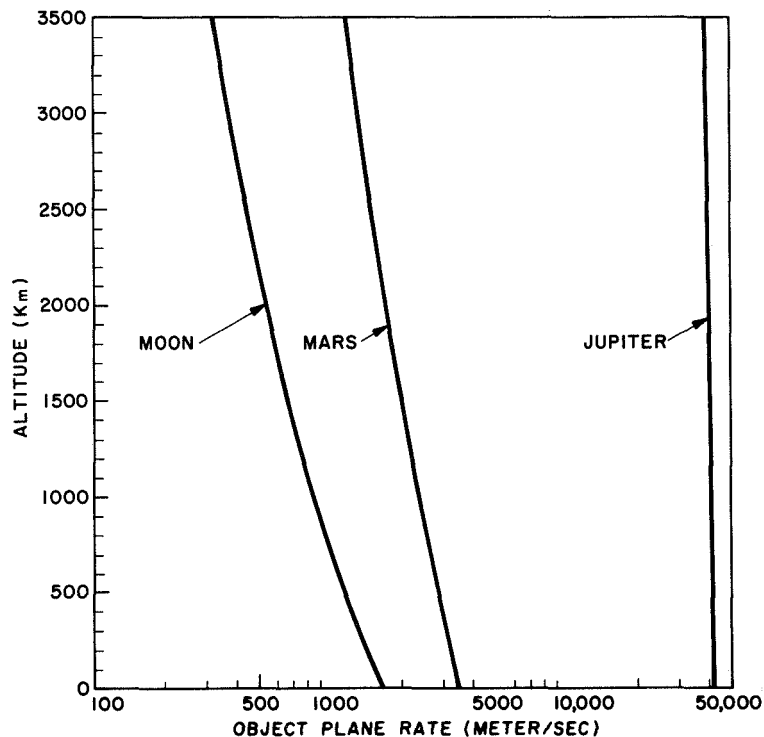orbit.

Figure 23.- Apparent northerly object plane motion
due to spacecraft orbital motion

Assume that the imaging system has a resolution of 2000 lines.
Table X shows that the lowest altitude quantum level above (say) 200
km has a quantum number K = 18 and lies at about 250 km above the
mean Martian equator. Thus it will take 18 Martian diurnal periods
(about 18.5 Earth days) for one complete coverage. The orbital
period of the spacecraft is 111.27 minutes. From Figure 8, we note
that a nadir pointing system is permissible and that the resulting
field of view should be 22.5 degrees.

It is assumed that the schematic of Figure 15 (including an
inertial measurement unit) represents the class of guidance and con-
trol instrumentation to be used aboard the spacecraft. If the position
of the spacecraft in the Martian orbit cannot be known to better than
400 m (after appropriate post-flight filter processing), then Figure
17 indicates that the accuracy of the attitude reference should not
degrade below 115 arcseconds (about 2 arcminutes).

With an orbital period of about 110 minutes, a complete pass over
the illuminated hemisphere will take 55 minutes. If alignment is
achieved just prior to passage over the pole and not corrected during
the next 55 minutes (one possibility, as determined by the actual
instrumentation to be employed), then Figure 19 shows that initial
alignment must be to the order of one arcminute and gyro drift rates
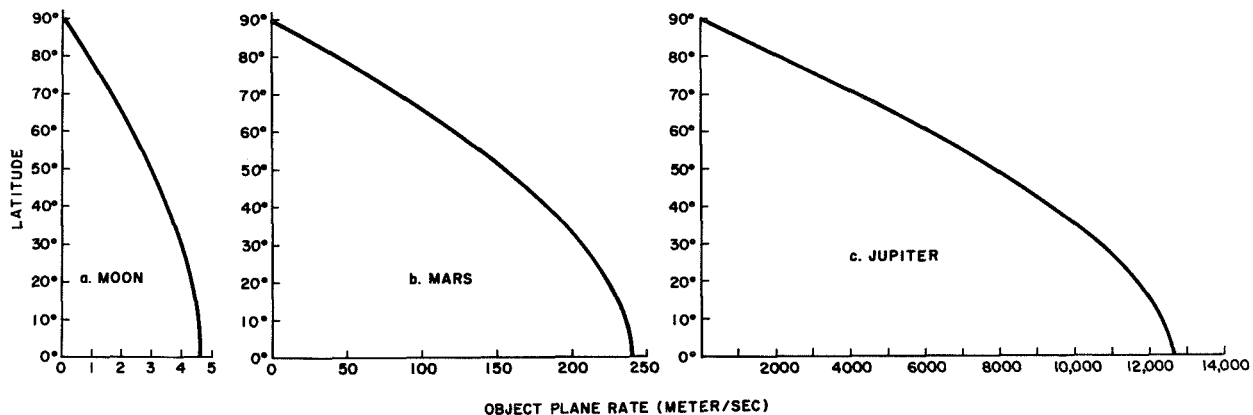should be bounded at about 0.05 deg/hr.

40

Figure 24.- Easterly object plane motion due to diurnal rotation

Equation (27) yields a maximum permitted amplitude of camera rotation about the yaw axis of about 2-3/4 degrees. Pitch and roll angular deviations, however, have maximum bounds of about 1 degree (from Figure 20 with a 22.5-deg field-of-view).

Image motion due to spacecraft attitude motion is small. Translational rates at the edge of the field due to 0.01 deg/sec yaw rate are about 12 m/sec (Figure 21). A similar pitch or roll rate will result in about 45 m/sec of image motion (Figure 22). However, the spacecraft's orbital motion results in an apparent object plane motion of almost 3200 m/sec (Figure 23) and Mars diurnal rotation produces an easterly motion of up to 240 m/sec (Figure 24b).

The foregoing results then may be used to initiate a detailed study of the selected mission and provide an indication of computer sizing and instrumentation tradeoffs upon which to base such a study.

V. CONCLUSIONS

The results of a preliminary study of the guidance and control requirements of planetary cartography are presented in this report. The parametric formulation of the imaging process in terms of mapping scale, image resolution, spacecraft altitude, and camera field-of-view permitted analyses of general validity over a range of missions. Orbit selection rules were derived which meet the requirement for complete and unique mapping coverage of the various planets (as limited only by orbital inclination). Detailed guidance and attitude control limitations were established for $1:10^6$ scale mapping of the Moon and Mars and $1:5 \times 10^6$ scale mapping of Mars and Jupiter. These results were discussed in terms of representative instrumentation subsystems.

The above-mentioned items form one product of the study. Another product, possibly of equal importance, was the definition of associated problems; an identification of "unanswered questions", and a listing of those areas of study which would require further elaboration when considering the design of a specific spacecraft system. A listing of

such items for additional study includes (although not necessarily in order of important):

1. A determination of anticipated tracking accuracy in terms of basic DSIF limitations and estimated uncertainties in the models of the various relevant gravitational fields

2. The prediction of the deviations (perturbations) to be experienced by a spacecraft in planetary orbit (after the methods of Karrenberg, Levin and Lüders)

3. Practical considerations of the attitude alignment operation.

4. An inclusion of actual planet geometry (inclination, orientation, orbital motion, orbital shape) in studies of illumination levels and mapping coverage

5. Needed data-rates will establish the type(s) of communication link(s) to be specified for given missions. Thus the expected data densities, data transmission and processing techniques and the data link transducer pointing problems need to be studied.

6. Planetary horizon sensors and surface feature trackers do not yet exist. Necessary to any such component development would be the analysis of the various models of planetary atmospheres in order to identify particular invariant horizon signatures.

Effort should be directed toward each of the above problem areas (and others as they evolve) if specific guidance and control requirements are to be established and corresponding instrumentation developed for selected mapping missions. A technological base would then result which would permit the cartographic operations described in this study.

REFERENCES

1. NASA 1965 Summer Conference on Lunar Exploration and Science, NASA SP-88, National Aeronautics and Space Administration, Washington, D. C., 1965.

2. 1967 Summer Study of Lunar Science and Exploration, NASA SP-157, National Aeronautics and Space Administration, Washington, D. C., 1967.

3. Moskowitz, S.; and Heinbockel, J.: Precision Pointing Control of Orbiting High-Resolution Photographic Systems. Presented at AIAA Guidance, Control, and Flight Dynamics Conference, Pasadena, Calif., August 12-14, 1968.

4. Doyle, F. J.: Photogrammetric Geodesy on the Moon. Annual Meeting, American Society of Photogrammetry, March 1968.

5. Bashe, R.; and Kennedy, S.: Martian Orbital Photographic Mission and System Analysis. Presented at 14th Annual Meeting, American Astronautical Society, Dedham, Mass., May 15, 1968.

6. Heacock, R. L.: Lunar Photography-Techniques and Results. Space Science Reviews, Vol. 8 (1968) pp. 214-257, O. Reidel Publishing Co., Dordrecht, Holland.

7. Kendrick, J. B., ed.: TRW Space Data (3rd edition): TRW Systems Group, Redondo Beach, Calif., 1967.

8. Michaux, C. M.: Handbook of the Physical Properties of the Planet Mars. NASA SP-3030, 1967.

9. Michaux, C. M.: Handbook of the Physical Properties of the Planet Jupiter. NASA SP-3031, 1967.

10. Karrenberg, H. K.; Levin, E.; and Lüders, R. D.: Orbit Synthesis. Air Force Report SAMSO-TR-68-341, Aerospace Corp., El Segundo, Calif., June 1968.

FIRST CLASS MAIL
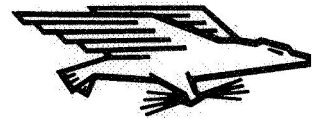
```
04U 001 39   51 3CS          70151  00903
AIR FORCE WEAPONS LABORATORY /WLOL/
KIRTLAND AFB, NEW MEXICO   87117


ATT E. LOU BOWMAN, CHIEF,TECH. LIBRARY
```

"The aeronautical and space activities of the United States shall be conducted so as to contribute . . . to the expansion of human knowledge of phenomena in the atmosphere and space. The Administration shall provide for the widest practicable and appropriate dissemination of information concerning its activities and the results thereof."

— NATIONAL AERONAUTICS AND SPACE ACT OF 1958

NASA SCIENTIFIC AND TECHNICAL PUBLICATIONS

TECHNICAL REPORTS: Scientific and technical information considered important, complete, and a lasting contribution to existing knowledge.

TECHNICAL NOTES: Information less broad in scope but nevertheless of importance as a contribution to existing knowledge.

TECHNICAL MEMORANDUMS: Information receiving limited distribution because of preliminary data, security classification, or other reasons.

CONTRACTOR REPORTS: Scientific and technical information generated under a NASA contract or grant and considered an important contribution to existing knowledge.

TECHNICAL TRANSLATIONS: Information published in a foreign language considered to merit NASA distribution in English.

SPECIAL PUBLICATIONS: Information derived from or of value to NASA activities. Publications include conference proceedings, monographs, data compilations, handbooks, sourcebooks, and special bibliographies.

TECHNOLOGY UTILIZATION PUBLICATIONS: Information on technology used by NASA that may be of particular interest in commercial and other non-aerospace applications. Publications include Tech Briefs, Technology Utilization Reports and Notes, and Technology Surveys.

Details on the availability of these publications may be obtained from:

SCIENTIFIC AND TECHNICAL INFORMATION DIVISION

NATIONAL AERONAUTICS AND SPACE ADMINISTRATION
Washington, D.C. 20546